AGU PUBLICATIONS

JGR

Journal of Geophysical Research: Biogeosciences

RESEARCH ARTICLE
10.1002/2014JG002798

Key Points:
- Disequilibrium assumption causes 1951–2010 NBP in US forests to vary
- Uncertainties related to nondisturbances have small impacts on NBP estimation
- Equilibrium assumption for initialization is acceptable for 1951–2010 estimation

Supporting Information:
- Texts S1–S4
- Tables S1–S3

Correspondence to:
F. Zhang,
fmin.zhang@utoronto.ca

Citation:
Zhang, F., J. M. Chen, Y. Pan, R. A. Birdsey, S. Shen, W. Ju, and A. J. Dugan (2015), Impacts of inadequate historical disturbance data in the early twentieth century on modeling recent carbon dynamics (1951–2010) in conterminous U.S. forests, *J. Geophys. Res. Biogeosci.*, *120*, 549–569, doi:10.1002/2014JG002798.

Received 10 SEP 2014
Accepted 9 FEB 2015
Accepted article online 22 FEB 2015
Published online 31 MAR 2015

Impacts of inadequate historical disturbance data in the early twentieth century on modeling recent carbon dynamics (1951–2010) in conterminous U.S. forests

Fangmin Zhang[1,2], Jing M. Chen[2], Yude Pan[3], Richard A. Birdsey[3], Shuanghe Shen[1], Weimin Ju[4], and Alexa J. Dugan[3]

[1]Collaborative Innovation Center on Forecast and Evaluation of Meteorological Disasters, College of Applied Meteorology, Nanjing University of Information Science and Technology, Nanjing, China, [2]Department of Geography, University of Toronto, Toronto, Ontario, Canada, [3]USDA Forest Service, Newtown Square, Pennsylvania, USA, [4]International Institute for Earth System Science, Nanjing University, Nanjing, China

Abstract Stand age and disturbance data have become more available in recent years and can facilitate modeling studies that integrate and quantify effects of disturbance and nondisturbance factors on carbon dynamics. Since high-quality disturbance and forest age data to support forest dynamic modeling are lacking before 1950, we assumed dynamic equilibrium (carbon neutrality) for the starting conditions of forests with unknown historical disturbance and forest age information. The impacts of this assumption on forest carbon cycle estimation for recent decades have not been systematically examined. In this study, we tested an assumption of disequilibrium conditions for forests with unknown disturbance and age data by randomly assigning ages to them in the model initial year (1900) and analyzed uncertainties for 1951–2010 carbon dynamic simulations compared with the equilibrium assumption. Results show that with the dynamic equilibrium assumption, the total net biome productivity (NBP) of conterminous U.S. forests was 188 ± 60 Tg C yr^{-1} with 185 ± 56 Tg C yr^{-1} in living biomass and 3 ± 23 Tg C yr^{-1} in soil. The C release due to disturbance on average was about 68 ± 55 Tg C yr^{-1}. The disequilibrium assumption causes annual NBP from 1951 to 2010 in conterminous U.S. forests to vary by an average of 13% with the largest impact on the soil carbon component. Uncertainties related to nondisturbance factors have relatively small impacts on NBP estimation (within 10%), while uncertainties related to disturbances cause biases in NBP of 4 to 28%. We conclude that the dynamic equilibrium assumption for the model initialization in 1900 is acceptable for simulating 1951–2010 forest carbon dynamics as long as disturbance and age data are reliable for this later period, although caution should be taken regarding the prior-1950 simulation results because of their greater uncertainties.

1. Introduction

Forest ecosystems are net carbon (C) sinks for atmospheric CO_2 and are the largest sinks among terrestrial ecosystems [*Pan et al.*, 2011a]. In recent decades, changing climate (increasing temperature and droughts) and atmospheric pollution (ozone, nitrogen (N) deposition, and rising CO_2 concentration) have had significant effects on forest C dynamics [*Pan et al.*, 2009; *Zscheischler et al.*, 2014]. At the same time, disturbances such as wildfires [*Wiedinmyer and Neff*, 2007], insect attacks [*Kurz et al.*, 2008], and harvesting have increased. These factors are likely to influence the atmospheric CO_2 concentration [*Schimel et al.*, 2000] over years or decades, either positively or negatively, by regulating the amount of C emitted to the atmosphere directly from damage to forest biomass and the rate of tree regeneration and soil decomposition in the years following disturbance events [*Boerner et al.*, 2008; *Running*, 2008; *Zeng et al.*, 2009]. Furthermore, forest stand age itself is another important factor influencing forest C dynamics [*Bradford and Kastendick*, 2010] (http://www.sciencedaily.com/releases/2014/07/140720204326.htm). Therefore, the quantification of these different forcing factors, and their relative impacts and uncertainties, is critical to understanding the forest C cycle and its future projections, which are becoming increasingly a focus in global C cycle research and a consideration in climate mitigation policy.

Biogeochemical models are useful tools to investigate how forests respond to different environmental variables and to enrich our current understanding of climate system-C cycle interactions. Most of these models share a similar structure and two essential components [*Weng and Luo*, 2011]: (1) C is fixed by plant

photosynthesis and allocated to multiple plant and soil C pools and (2) C transfers among pools are regulated by environmental variables. Thanks to increasing availability of stand age and disturbance data in recent years, some regional modeling studies have started to integrate disturbances with other processes of forest C cycles to evaluate ecosystem responses to global change on decadal and century time scales at the global or regional levels [*Chen et al*., 2000a; *Masek and Collatz*, 2006; *Williams et al*., 2012; *Zhang et al*., 2012a]. However, due to a lack of current and historical information about forest ecosystem disturbances within the modeling domain, an assumption of an equilibrium state for a historical time is often made for estimating initial C pools [*Carvalhais et al*., 2010]. For process-based models, a common initialization method is to run the models repeatedly with climate conditions of a preindustrial period until ecosystems reach a dynamic equilibrium state, i.e., net C exchange approaches zero at an annual scale [*Morales-Nin et al*., 2005; *Chen et al*., 2003; *Zhang et al*., 2012a]. However, it has been reported that the application of the equilibrium assumption for model initialization to the ecosystems in a disequilibrium state may result in systematically inconsistent estimates of C stocks in the subsequent years [*Pietsch and Hasenauer*, 2006; *Wutzler and Reichstein*, 2007; *Carvalhais et al*., 2010].

The Integrated Terrestrial Carbon Cycle Model (InTEC) is a process-based biogeochemical model embedding some empirical equations for simulating long-term ecological processes. The advantage of this model is that it integrates the effects of both nondisturbance factors (climate, CO_2 concentration, and N deposition) and disturbances with stand age information on long-term forest C dynamics [*Chen et al*., 2000, 2000a, 2000b, 2003; *Ju et al*., 2007; *Zhang et al*., 2012a]. We previously evaluated the relative contributions of both forest disturbance and nondisturbance factors on the net C changes of conterminous U.S. forests [*Zhang et al*., 2012a] from 1951 to 2010. However, forests with unknown disturbance history and stand age information prior to 1950 account for more than 50% of the total forest area across the conterminous U.S. and up to 75% in 1900. Similar to other biogeochemical models, we assumed that forests were in a dynamic equilibrium state for the period prior to the known stand age and disturbance trajectories [*Zhang et al*., 2012a]. However, the importance of this assumption in C cycle simulations for recent decades remains a significant question.

Based on our previous work [*Zhang et al*., 2012a], the goal of this study is to examine if simulation of U.S. forest C sinks or sources in recent decades from 1951 to 2010 (especially after 1990) is significantly affected by the shortage of disturbance and stand age information prior to 1950. We further investigate the relative magnitudes of the contributions of disturbance and nondisturbance factors to the C sink estimation which could be affected by the dynamic equilibrium assumption and whether uncertainties in other input data would have significant impacts on the modeling results in recent decades. Based on our evaluation of uncertainties in C sink estimation due to assumptions in model structure versus input data, we update C sink and source estimation for U.S. forests from 1951 to 2010 [*Zhang et al*., 2012a].

2. Data and Modeling Methodology

2.1. Overview of the Modeling Approach

Net primary production (NPP) is affected by disturbances, stand age, climate, and atmospheric composition, and the C dynamics of a forest region are a function of these forcing factors through their aggregated influence on landscape patches [*Chen et al*., 2000b]. These factors are grouped into disturbance and nondisturbance factors in our study (Figure 1). Disturbance factors that we simulate include fire, harvesting, and insect outbreaks, which determine forest stand age and regrowth, while nondisturbance factors include climate, atmospheric CO_2 concentration, and N deposition.

In the InTEC model, we integrate the effects of nondisturbance and disturbance factors since the initial year (1900). The historical C dynamics are estimated progressively through a mechanistic aggregation of disturbance and nondisturbance factors starting from 1900 [*Chen et al*., 2003]. C dynamics in the whole forest system were divided into 13 individual components, which are summarized as living biomass and soil (the nonliving biomass) C pools (Figure 1).

Disturbances are explicitly considered as processes that release a C pulse into the atmosphere and modify the terrestrial C balance in the disturbance year and the subsequent years. Forest stands are assumed to begin tree regrowth immediately after disturbance, and then aging of stands affects the C dynamics over time. Disturbance information used in this study was derived from the U.S. Forest Inventory and Analysis (FIA) data

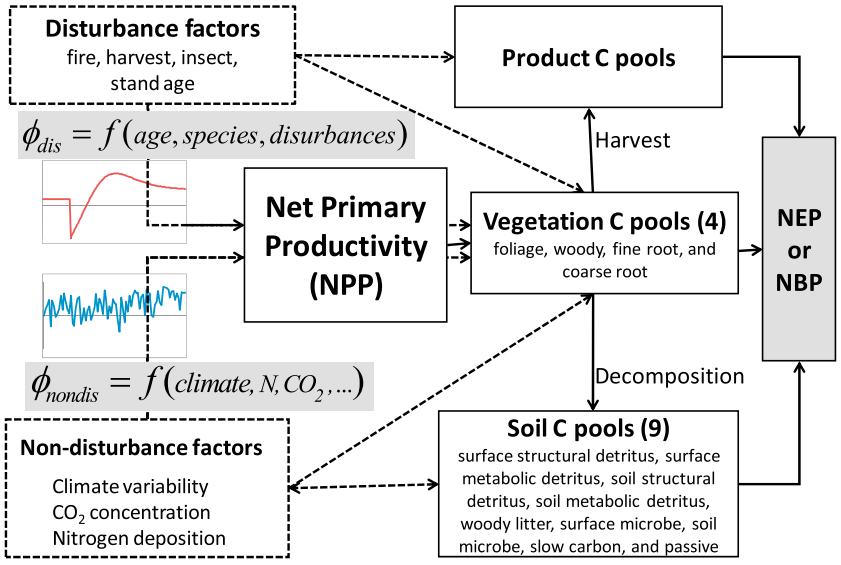

Figure 1. Conceptual scheme of the carbon (C) cycle in the Integrated Terrestrial Carbon Cycle Model (InTEC). Solid arrows indicate C flow, and dashed arrows indicate influences. $\phi_{dis}(i)$: disturbance function; $\phi_{nondis}(i)$: non-disturbance function; NEP: net ecosystem productivity; and NBP: net biome productivity. NPP is equal to the difference between the photosynthetic rate and autotrophic respiration of plants. NEP is equal to the sum of NPP and the C loss to the atmosphere via heterotrophic respiration. NBP is equal to the sum of NEP and C fluxes associated with nonrespiratory losses due to disturbances such as combustion from fire or export to external pools following harvesting. If no disturbances occur in a given year, NBP equals to NEP.

and recent Moderate Resolution Imaging Spectroradiometer (MODIS) observations, the Landsat Ecosystem Disturbance Adaptive Processing System, and the Monitoring Trends in Burn Severity (MTBS) data, all of which are insensitive to partial harvesting, thinning, and low-intensity natural disturbances [*Masek et al*., 2008; *He et al*., 2011]. Thus, disturbance areas are defined as those affected only by stand-replacing disturbances, and partially harvested or disturbed stands are treated as undisturbed stands, following a similar treatment in *Williams et al*. [2012]. A stand age map developed by *Pan et al*. [2011a] is used to determine the timing of the last stand-replacing disturbances. To include the effects of multiple disturbances in recent years, we compiled annual disturbance maps since 1984 for the conterminous U.S. and then modeled multiple disturbances in each 1 km grid cell since 1984. For the period prior to the known stand age and recent disturbance trajectories, we assume that forests were in a dynamic equilibrium state at an age dubbed "equilibrium age" [*Chen et al*., 2003] in our previous study [*Zhang et al*., 2012a].

The equilibrium age is defined by the available NPP-age curves, i.e., the equilibrium age is the year when NPP of a stand reaches an asymptotic value and is balanced by heterotrophic respiration so that the stand is C neutral, an equilibrium state. However, it is possible that this equilibrium assumption could introduce large differences in results compared to our historical C dynamics modeling when a stand was disturbed prior to the period with known stand age. Therefore, we investigated the possible range of these uncertainties by randomly assigning different stand ages to pixels having a single disturbance, forcing forests in an assumed dynamic equilibrium state to an initial disequilibrium state (see section 2.3 for details).

2.1.1. Model Description

The InTEC model is a process-based biogeochemical model driven by monthly climate data, vegetation parameters, and forest disturbance information to estimate annual forest C and N fluxes and C pools at regional scales. The model is a combination of a modified CENTURY model for soil C and nutrient dynamics [*Parton et al*., 1987], the N mineralization model of *Townsend et al*. [1996], a canopy-level annual photosynthesis model developed from Farquhar's leaf biochemical model [*Farquhar et al*., 1980] using a temporal and spatial scaling scheme [*Chen et al*., 1999, 2000a, 2000b], a three-dimensional distributed hydrological model for simulating soil moisture and temperature [*Ju and Chen*, 2005], and NPP-age relationships derived from forest inventory data [*He et al*., 2012]. As the modeling strategy of InTEC is quite different from the previous versions of the model [*Chen et al*., 2000, 2000a, 2000b, 2003; *Ju et al*., 2007], the key characteristics of C-related modules are outlined here.

2.1.1.1. Calibrating NPP

In theory, NPP changes with climate variability, atmospheric CO_2 concentration, N deposition, disturbances, stand age, etc. Functions of $\phi_{NPPn}(i)$ and $\phi_{NPPd}(i)$ in year (i) are used to describe the corresponding accumulated nondisturbance and disturbance effects since the beginning year. Thus, NPP in year i is progressively calculated by [*Chen et al*., 2000a]

$$NPP(i) = NPP_0 \times \phi_{NPPn}(i) \times \phi_{NPPd}(i), \tag{1}$$

NPP_0 is the initial value of NPP in the starting simulation year. With known values of $\phi_{NPPn}(i)$ and $\phi_{NPPd}(i)$ and NPP(i), NPP_0 can be determined retrospectively.

The fine-tuned NPP_0 is derived by retrospectively reconstructing the historical NPP values back to the beginning year according to NPP in a recent reference year, e.g., to calibrate NPP for each grid cell, NPP_0 is iteratively adjusted until the difference between the calculated NPP(i) and the NPP value in the reference year i is smaller than ±1%. If NPP_0 and $\phi_{NPPn}(i)$ and $\phi_{NPPd}(i)$ are known for each grid, the values of NPP(i) in historical year i can be calculated. The fine-tuned NPP_0 is in turn used to adjust our initialized C pools in the beginning year and together with the fine-tuned C pools is used to simulate the real transient and historical C dynamics for each spatial grid cell.

2.1.1.2. Nondisturbance Effects on NPP

The leaf-level instant photosynthesis rate (P_l) is calculated by Farquhar's biochemical model [*Farquhar et al*., 1980] and scaled up to the canopy photosynthesis rate P_{can} using the sunlit and shaded leaf separation method of *Chen et al*. [1999]. The area-averaged annual gross primary product (GPP) in year i over the area (A_i) of the aggregated forest regions (y) and time period (t) of photosynthesis can be calculated by

$$GPP(i) = \frac{1}{A_t}\int_t\int_y P_{can}(y,t)\mathrm{d}y\mathrm{d}t. \tag{2}$$

The changes of GPP are calculated using a relationship between the interannual variability and the external forcing factors [*Chen et al*., 2000a]:

$$\frac{\mathrm{dGPP}(i)}{\mathrm{d}i} = \int_t P_{can}(y,t)\frac{\partial y}{\partial i}\mathrm{d}t + \int_y P_{can}(y,t)\frac{\partial l_g(t)}{\partial i}\mathrm{d}y + \int_t\int_y \mathrm{d}P_{can}(y,t)\mathrm{d}y\mathrm{d}t. \tag{3}$$

The first term represents the effects caused by changes in forest areas, the second term the effects caused by the changes of growing season length (l_g), and the third term the effects on annual GPP changes caused by accumulated changes in $P_{can}(y,t)$. Details on how to calculate these three terms can be found in *Chen et al*. [2000a].

Using a three-step spatial and temporal scaling algorithm and a set of differential equations, the interannual relative change in GPP ($\frac{\mathrm{dGPP}}{\mathrm{d}i}$) is calculated as

$$\frac{\mathrm{dGPP}(i)}{\mathrm{d}i} = \chi(i)\left[\frac{\mathrm{GPP}(i)+\mathrm{GPP}(i-1)}{2}\right], \tag{4}$$

and GPP is derived as

$$GPP(i) = GPP(i-1)\frac{2+\chi(i)}{2-\chi(i)} = GPP(i-1)\phi_{GPPn}(i), \tag{5}$$

where $\phi_{GPPn}(i)$ is the integrated effects of nondisturbance factors on GPP; $\chi(j)$ is a function of climate variables, atmospheric CO_2 concentration, growing season length, N content, soil temperature, and soil available water on P_{can}. The deviations of $\chi(j)$ are summarized in Text S1 in the supporting information.

Annual NPP of a forest region in year i is calculated as

$$NPP(i) = GPP(i) - R_a(i), \tag{6}$$

where $R_a(i)$ is annual autotrophic respiration by plants (see Text S2 in the supporting information for details). Using the interannual relative change in $NPP(i-1)$, annual NPP(i) can be calculated [*Ju et al*., 2007] alternatively as

$$NPP(i) = NPP(i-1)\frac{1+B(i)}{1-B(i)} = NPP(i-1)\phi_{NPPn}(i), \tag{7}$$

$$\begin{aligned} B(i) &= \frac{NPP(i)-NPP(i-1)}{NPP(i)+NPP(i-1)} = \frac{GPP(i)-GPP(i-1)-R_a(i)+R_a(i-1)}{GPP(i)+GPP(i-1)-R_a(i)-R_a(i-1)}, \\ &= (X(i)-1)-\beta(i-1)\left(\frac{Y(i)-1}{(X(i)+1)}-\beta(i-1)(Y(i)+1)\right. \end{aligned} \tag{8}$$

where $\phi_{NPPn}(i)$ is the integrated effects of nondisturbance factors on NPP; $X(i)$ is the interannual variability of GPP between year i and year $i-1$, which is calculated by equations (2)–(5); $\beta(i-1)$ is the ratio of respiration to GPP in year $i-1$; and $Y(i)$ is the interannual variability of autotrophic respiration rate between year i and year $i-1$.

2.1.1.3. Disturbances

2.1.1.3.1. Disturbance Effects on NPP

Disturbances affect NPP over a landscape by altering age-class distributions and forest areas. Given forest areas $A(x, i)$ at stand ages x in a given year i, the overall effect of disturbances on NPP is then given by [*Chen et al*., 2000a]

$$\phi_{NPPd}(i) = \int_0^{\infty} F_{npp}(x)A(x,i)\mathrm{d}x \Big/ \int_0^{\infty} F_{npp}(x)A(x,0)\mathrm{d}x, \tag{9}$$

where F_{npp} derived by NPP-age curves represents normalized NPP factors, defining the forest growth pattern for each forest species.

2.1.1.3.2. C Emission Due To Disturbances

The total amount of C release ($D(i)$) at the time of disturbance events in year (i) is estimated by

$$D(i) = D_{fire}(i) + D_{harvest}(i) + D_{insect}(i), \tag{10}$$

where $D_{fire}(i)$, $D_{harvest}(i)$, and $D_{insect}(i)$ are the amounts of C release due to fire, clear-cut harvesting, and insect-induced mortality, respectively.

During the simulation period of this study, all C emissions were assumed to be caused by either fire or harvest due to a shortage of spatially explicit data sets about the severity of damage of insect-impacted forests. Insect infestations were treated the same as harvested forests, since stand-replacing insect disturbances may have similar impacts on ecosystem dynamics except for producing a larger deadwood pool which would emit C or increase soil C pools in the subsequent years. In a disturbance year, we estimated the C from harvested wood products from harvest volume data [*Ince*, 2000; *Adams et al*., 2006; *Smith et al*., 2009] using the methods of *Smith et al*. [2006]. For simplicity, average conversion parameters from volume to C density were used within a given region although they were suggested to be different among forest types within the same regions [*Smith et al*., 2006]. Otherwise, forests experienced a pulse of C losses from fires. The amount of C directly emitted from fire is estimated as the sum of 100% of foliage C, 25% of woody C, and 100% of C in surface structural and metabolic detritus pools [*Kasischke et al*., 2000]. The remaining biomass C is transferred to woody litter, surface metabolic detritus, and surface structural detritus [*Chen et al*., 2003]. After disturbances, forest stands start to regenerate immediately in the following year, and after a relatively short period of net C emissions, net C change becomes positive and reaches a peak as plants regenerate and soil detritus decays. Figure 2 showed the changes of disturbed areas from fire, harvest, insect, and C releases directly from the disturbance event as estimated by InTEC. Compared with a recent inventory of U.S. greenhouse gases [*Environmental Protection Agency* (*EPA*), 2009], InTEC can estimate C emission reasonably well for recent years but might underestimate it in the early twentieth century (pre-1950) due to the inadequate disturbance information.

2.1.1.4. C Fluxes and Pools

The InTEC model stratifies living biomass C into four pools (foliage, woody, fine root, and coarse root) and nonliving biomass C into nine pools (surface structural litter, surface metabolic litter, soil structural litter, soil metabolic litter, woody litter, surface microbe, soil microbe, slow C, and passive C) (Figure 1). Biomass C pools are conceptualized as a function of the existing C pool sizes, allocation from current NPP, turnover to soil C pools, and C releases to the atmosphere during disturbance events. The soil C pools are a function of the existing soil pool sizes, turnover from biomass C pools, and various abiotic factors (soil temperature, soil moisture, and soil texture) that modulate the decomposition of each soil C pools in a unique manner. The sizes of the various C pools for each year are determined by solving a set of equations [*Chen et al*., 2000a]:

$$C_j(i) = C_j(i-1) + \Delta C_j(i), \tag{11a}$$

$$\Delta C_{vegetation,j}(i) = f_j(i)\mathrm{NPP}(i) - k_j(i)C_j(i) - \frac{\varepsilon_j A(i)}{A_t}, \tag{11b}$$

$$\Delta C_{soil,j}(i) = \sum_{m=1}^{13} \varepsilon_{m,j}\zeta_{m,j}(i)C_m(i-1) - \zeta_j C_j(i) - \xi_j C_j(i), \tag{11c}$$

where $\Delta C_j(i)$ is the jth C pool change in the ith year; annual NPP(i) is allocated to four biomass C pools in foliage, woody, coarse root, and fine root; f_j is the allocation coefficient of NPP to the jth biomass pool for

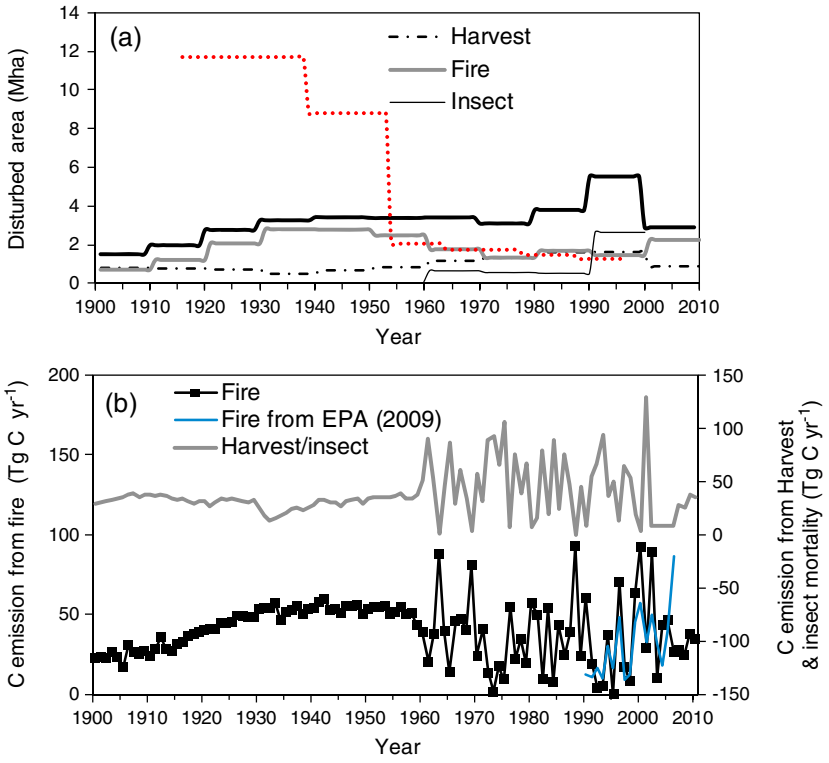

Figure 2. Forest areas disturbed by disturbance types compared with fire estimated from *Birdsey and Lewis* [2002] prior to 1950 and the corresponding C emissions from fire and harvest + insect mortality from 1900s to 2000s compared with *EPA* [2009], respectively. For more information about disturbed areas by disturbance types, refer to Figure 3 in *Zhang et al.* [2012a].

different forest types; k_j is the turnover rate of the jth C pool ($C_j(i)$) to soil; $\frac{\varepsilon_j A(i)}{A_t}$ is the C loss from forest disturbances; ε_j is the C loss per unit disturbed forest in the jth C pool; $A(i)$ and A_t are disturbed and total forest area, respectively; and $\zeta_{m,j}$ is the weighted C transfer coefficient between mth and jth C pools. ζ_j and ξ_j are the weighted C transfer coefficients from the jth C pool to other C pools and the atmosphere. The calculations for each C pool change ΔC in disturbed and nondisturbed years summarized in Appendix A1 here.

The total annual ecosystem heterotrophic respiration ($R_h(i)$) is calculated as the sum of C released to the atmosphere during decomposition from nine soil C pools, i.e.,

$$R_h(i) = \sum_{m=1}^{9} k_{m,a}(i) C_m(i), \tag{12}$$

where $k_{m,a}$ is the rate of C released from the mth C pool to the atmosphere, which is a function of C pools and abiotic factors such as soil temperature, soil moisture, texture, N availability, and lignin content using a modified algorithm from the CENTURY model [*Ju et al.*, 2007]. The C pools are estimated as a function of NPP over a specified period of time, which has a direct relationship with stand age, and therefore, R_h is indirectly influenced by stand age.

The annual regional C balance is the sum of NBP of each pixel, which equals the difference between net ecosystem productivity (NEP) and C release from disturbances, that is,

$$\mathrm{NBP}(i) = \mathrm{NEP}(i) - D(i) = \mathrm{NPP}(i) - R_h(i) - D(i). \tag{13}$$

If there are no C losses due to combustion from fire or decomposition of abundant dead wood and detritus following disturbances such as harvesting and insect attack in a given year, NBP is equal to NEP.

After disturbances, forests start to recover immediately in the following year, and net ecosystem C changes may initially be negative but then become positive and reach a peak as vegetation recovers and the decay

ofsoil detritus declines. Biomass C that is not immediately released after a disturbance is transferred to corresponding soil structural, surface structural, and woody detritus C pools [*Zhang et al*., 2012a, Figure 1]. The dead tree C pool is transferred to the soil and then the heterotrophic respiration increases, although the increase is slow because of the long C residence time of coarse detritus.

2.1.1.5. Model Parameterization

The actual soil C pools are determined by constraining the decomposition rate and the turnover rate. Due to decomposition and allocation of C between vegetation and soil C pools, the size of each C pool changes with time. Scalars such as soil temperature, moisture, N availability, soil texture, and lignin contents constrain the decomposition and turnover rates [*Ju et al*., 2007]. The effect of soil moisture is calculated in a simplified manner by considering the annual precipitation, evapotranspiration, and soil hydraulic conditions. N fixation, mineralization, and immobilization alter the C:N ratio of each soil C pool, which in turn affects the uptake of C by plants. Parameters such as C allocation, turnover rates, and decomposition rates used for Canada and China were described in *Chen et al*. [2000, 2000a, 2000b], *Ju et al*. [2007], and *Govind et al*. [2011].

For U.S. forests, we adjusted previous InTEC parameters to fit to measured NEP at 35 sites (Figure A1 and Table A2) and compared the results with FIA data. The parameters used to describe C allocation, turnover rates, decomposition rates, and loss rates of C pools for the U.S. were described in the supporting information of *Zhang et al*. [2012a] and Appendix A here.

2.1.2. Model Inputs

A series of spatial and temporal data sets including disturbance information, stand age, climate, atmospheric CO_2 concentration, N deposition, soil, and reference NPP were used. All spatially coarse data were interpolated to 1 km resolution.

Monthly mean air temperature, relative humidity, and precipitation from 1901 to 2010 were interpolated from the 0.5° global data set (http://www.cru.uea.ac.uk/cru/data/) [*Harris et al*., 2014]. The data set was produced from available station observations by the UK Climate Research Unit (CRU3.0). Long-term 1948–2010 monthly solar irradiance data were from the T62 Gaussian reanalysis data by the U.S. National Center for Atmospheric Research. The pre-1948 monthly solar irradiance data for each grid cell were produced using temperature, humidity, and precipitation based on the Bristow-Campbell model [*Thornton and Running*, 1999].

Atmospheric CO_2 concentration from 1958 to 2010 is from monthly data measured at Mauna Loa Observatory (20°N, 156°W) (http://cdiac.esd.ornl.gov/ftp/trends/co2/maunaloa.co2) [*Keeling et al*., 2009]. The pre-1958 CO_2 data were extrapolated based on CGCM2 [*Flato and Boer*, 2001]. We assume no spatial variation in CO_2 concentration over the whole study region.

Spatially explicit N deposition data from 1979 to 2010 were interpolated by a kriging method from the concentration data collected at the monitoring sites of the National Atmospheric Deposition Project and National Trends Network (http://nadp.sws.uiuc.edu/data/) [*Pan et al*., 2009]. The 1 km estimates for each grid cell from 1978 back to 1901 were proportionally extrapolated based on historical greenhouse gas emissions and average N deposition data during 1990 and 2000 [*Zhang et al*., 2012a].

The stand age map, referenced to the year 2006 at 1 km resolution, was produced by combining the FIA data and optical remote sensing data [*Pan et al*., 2011b]. A mean stand age was used in each 1 km × 1 km cell grid. Stand age histograms for 1970, 1990, and 2006 show how stand age structures of U.S. forests changed with time in different regions (Figure 3). For example, in the south, more land area was occupied by younger forests (<50 years) in 1970. In 1990, middle age forests (30–60 years) are dominant across the U.S., whereas there were more young forests (<10 years) in the south region. In 2006, young and middle age forests (<90 years) were widely distributed in the north and south regions, while old forests (>150 years) are prominent in the Rocky Mountain and West Coast regions.

A forest disturbance map, developed from Monitoring Trends in Burn Severity (MTBS) data and the MODIS burned area product from 2000 to 2010, was used to identify recent fire disturbances from 1984 to 2010. We estimated the C release from harvested wood products based on FIA data [*Ince*, 2000; *Birdsey and Lewis*, 2002; *Adams et al*., 2006; *Smith et al*., 2006, 2009] in a disturbance year for each pixel. Estimates for nonsurvey years were derived by interpolation between two known points.

The U.S. forest-type classifications at 1 km resolution were based on 250 m Terra MODIS imagery and FIA plot data [*Ruefenacht et al*., 2008]. The Global Land Cover Map 2000 at 1 km resolution (GLC2000; http://www.

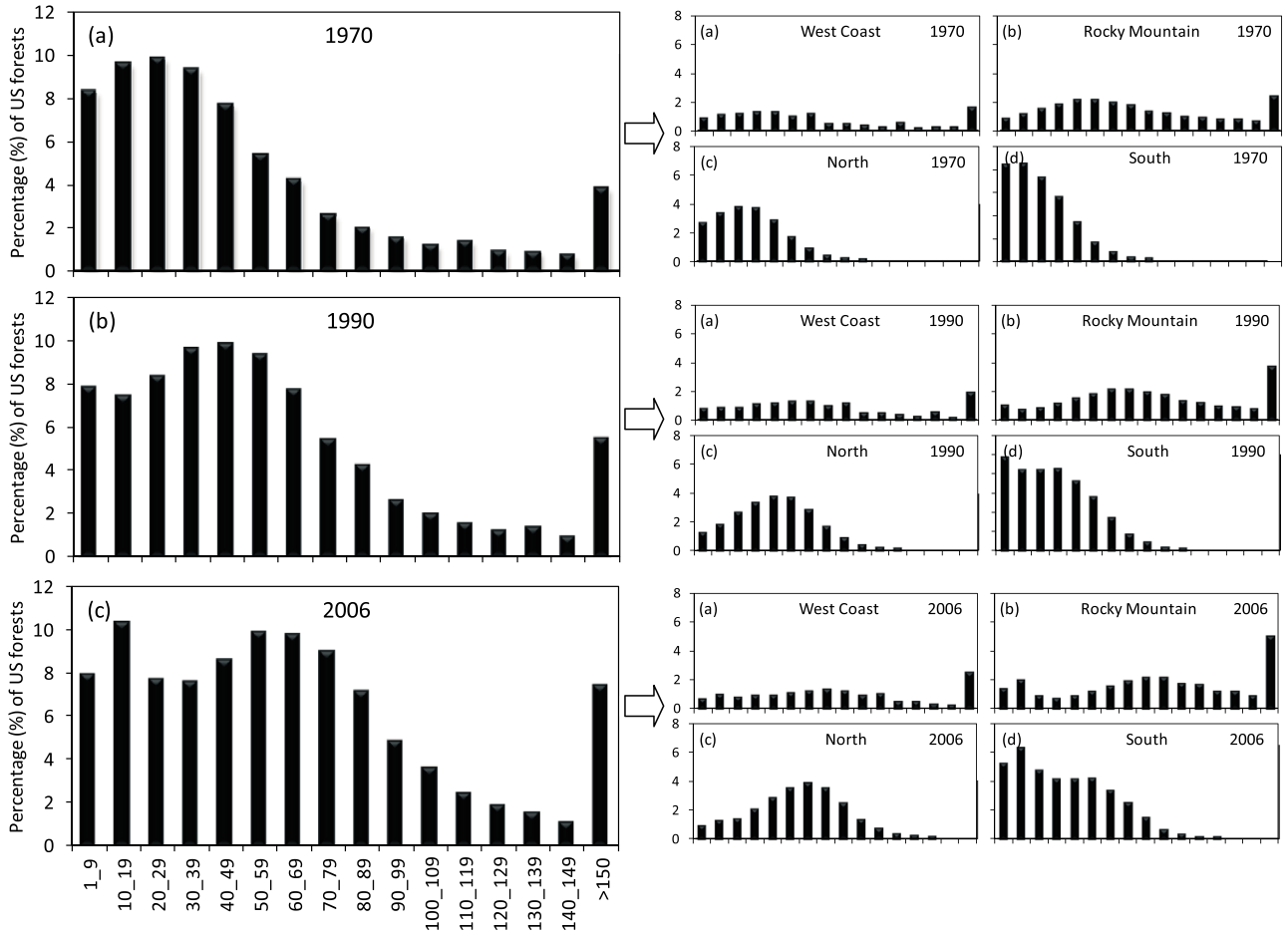

Figure 3. Histograms of the percentage of forest area at different stand ages in four regions across the conterminous U.S. forests. Regions are described in http://www.fs.fed.us/research/rpa/regions.php.

eogeo.org/GLC2000), produced using SPOT4 VEGETATION data, was used to distinguish the nonforest and forest areas.

The 1 km soil physical properties including soil depth and fractions of clay, silt, and sand were derived from the 0.0833° coarse data set from the International Geosphere-Biosphere Programme-Data and Information System (http://www.daac.ornl.gov).

The NPP product from the Boreal Ecosystem Productivity Simulator (BEPS) at 1 km resolution for 2003 derived from GPP [*Zhang et al.*, 2012b] was used as the benchmark to tune the initial NPP values in 1900 until NPP simulated agrees within 1% with BEPS NPP for each grid cell.

Eighteen NPP-age curves for the conterminous U.S. forests [*He et al.*, 2012] were used to calculate the normalized NPP factor (F_{npp}). To apply these relationships to the whole conterminous U.S., they were extrapolated to the actual ages available from the forest age map and normalized against their maximum NPPs in their forest life spans.

2.2. Model Validation

We validated the modeled state-to-state C stocks with estimates from FIA data [*Zhang et al.*, 2012a], which indicated that our estimates were within the range of inventory-based greenhouse gas reports for the U.S. compiled by the Environmental Protection Agency. In our previous paper [*Zhang et al.*, 2012a], we showed that our simulations of U.S. forest carbon sinks in recent years are within the range of the variability of previously published results [e.g., *Birdsey and Heath*, 1995; *Turner et al.*, 1995; *Birdsey and Lewis*, 2003; *Hurtt et al.*, 2002; *EPA*, 2009; *Williams et al.*, 2012].

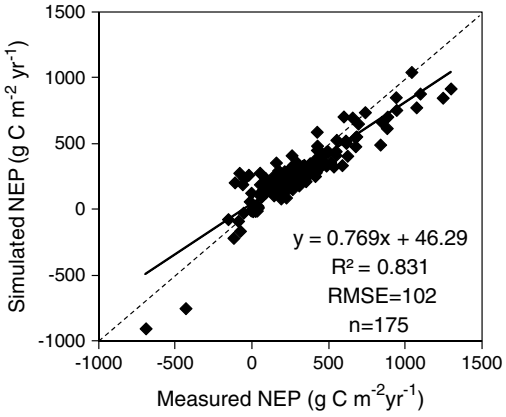

Figure 4. Comparison between modeled net ecosystem productivity (NEP) values with measurements at AmeriFlux sites using actual land cover, forest type, and stand age.

In this study, we validated our site-level model results against measured NEP at AmeriFlux sites. The AmeriFlux network provides invaluable eddy covariance (EC) data (http://ameriflux.ornl.gov) which are typically used to estimate net ecosystem exchange (NEE) between forests and the atmosphere. The 35 AmeriFlux sites representing a diversity of forest ecosystems and climate types were used for validating NEP estimates at sites where it could be assumed that negative NEE is approximately equal to NEP, i.e., those sites that were not disturbed during the eddy covariance observation period (see Appendix A3). Among these sites, 12 are dominated by young forests (age $<$ 20 years) and four sites are old forests (age $>$ 100 years).

The simulated NEP values, in general, agreed well with NEP ($-$NEE) measured at tower sites, except for some cases (Figure 4). The model captured 83.2% of the variance in NEP with root-mean-square error (RMSE) of 102 g C m^{-2} yr^{-1} and a slope of 0.77 relative to measured NEP. The differences between modeled and measured estimates at some flux tower sites, particularly at old forest sites, may be mostly caused by the heterogeneity within the modeled 1 km pixels, as the footprint of flux measurement in a pixel may not represent the average condition of the pixel. This is a common difference in comparisons between measurements at flux towers representing specific conditions and estimates at larger scales that represent the heterogeneity of the landscape.

2.3. Uncertainty Analysis Methods

A sensitivity analysis can determine the contributions of parameters to the overall model output uncertainty. In order to quantify the uncertainties in estimated NBP of U.S. forests, only the key parameters and inputs were considered here. The absolute error (σ, given as a standard deviation) and relative error (e, %) of total C changes from each key parameter and input are calculated [*Taylor*, 1997]:

$$\sigma^2{}_{\Delta C} = \sigma^2{}_{\text{disturbance}} + \sigma^2{}_{\text{age}} + \sigma^2{}_{\text{referenceNPP}} + \sigma^2{}_{\text{NPP-agecurves}} + \varepsilon, \tag{14a}$$

$$e_{\Delta C} = \frac{\sigma_{\Delta C}}{\Delta C}, \tag{14b}$$

where ε represents errors from interaction effects of all related parameters on each C changes.

It was estimated that about 15% of forests have indeterminate ages in the post-1980 period based on the stand age and disturbance maps used, but prior to 1950, forests with unknown ages increase to 50%. If the statistical estimates of disturbed forest areas due to fire are realistic [*Birdsey and Lewis*, 2002], then 1–4% of disturbances would be unintentionally ignored if there are no available spatial disturbance estimates (Figure 2). Because of insufficient historical disturbance and stand age data, we made an equilibrium assumption to initialize the model prior to the period with actual known disturbance and age information. The equilibrium age assumption for forests with unknown stand age prior to the year with known stand age or disturbance information may not fully account for possible disturbance effects on C dynamics. To evaluate the uncertainties from such an assumption, forests without known stand ages were randomly assigned to ages of 20, 60, 100, and 150 years as well as the current stand age in the beginning year (1900 in this simulation), respectively, which we called disequilibrium assumptions. Then the forests were randomly disturbed based on disturbed forest area percentages from historical statistics (Figure 2) [*Birdsey and Lewis*, 2002]. If forests were disturbed, stand

Table 1. Contributions of Nondisturbance and Disturbance Factors to the Annual Net Biome Productivity (NBP) in U.S. Forests During the Period of 1951–2010, Including Living Biomass (dCveg) and Soil (dCsoil; Nonliving Biomass) Components

(Tg C yr^{-1})	dCveg	dCsoil	NBP
Nondisturbance	22 ± 6	36 ± 1	58 ± 5
Disturbance	163 ± 56	(−37) ± 23	126 ± 60
Total	185 ± 56	3 ± 23	188 ± 60

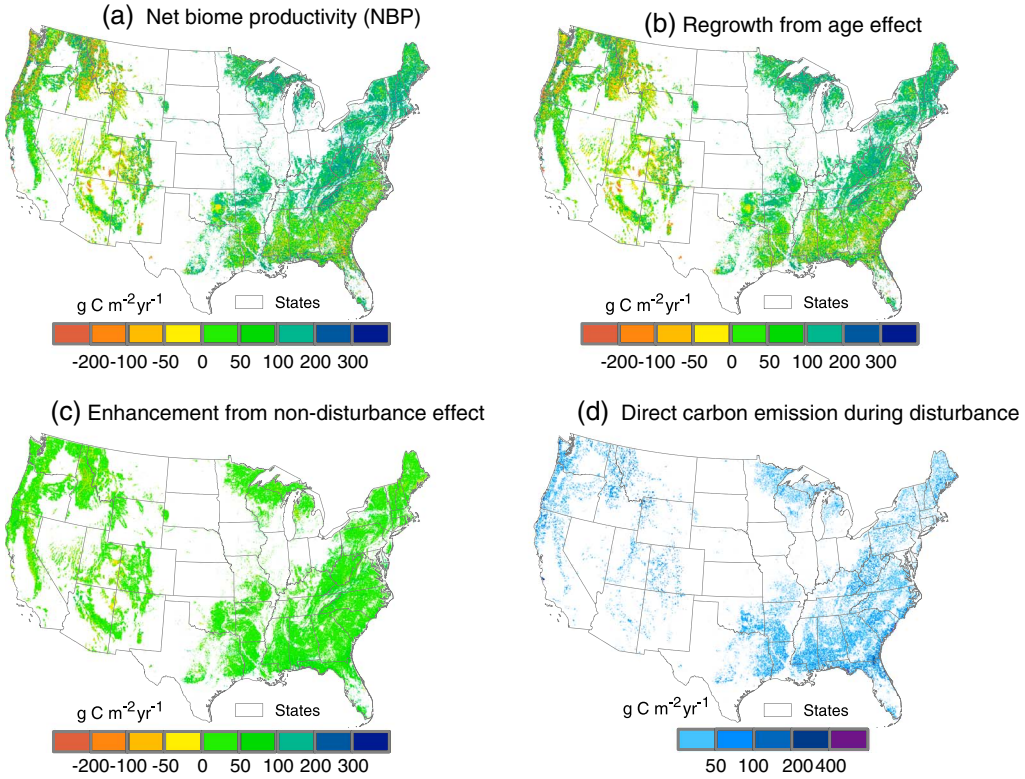

Figure 5. Spatial distribution of net biome productivity (NBP) in the conterminous U.S. forests averaged from 1951 to 2010 due to (a) overall effect, (b) regrowth, (c) nondisturbance factors, and (d) direct carbon (C) emission to the atmosphere due to disturbance (e.g., fire, harvest, and insects) in the disturbed years. (Positive values indicate sinks of C, and negative values indicate sources of C to the atmosphere in Figures 5a–5c.).

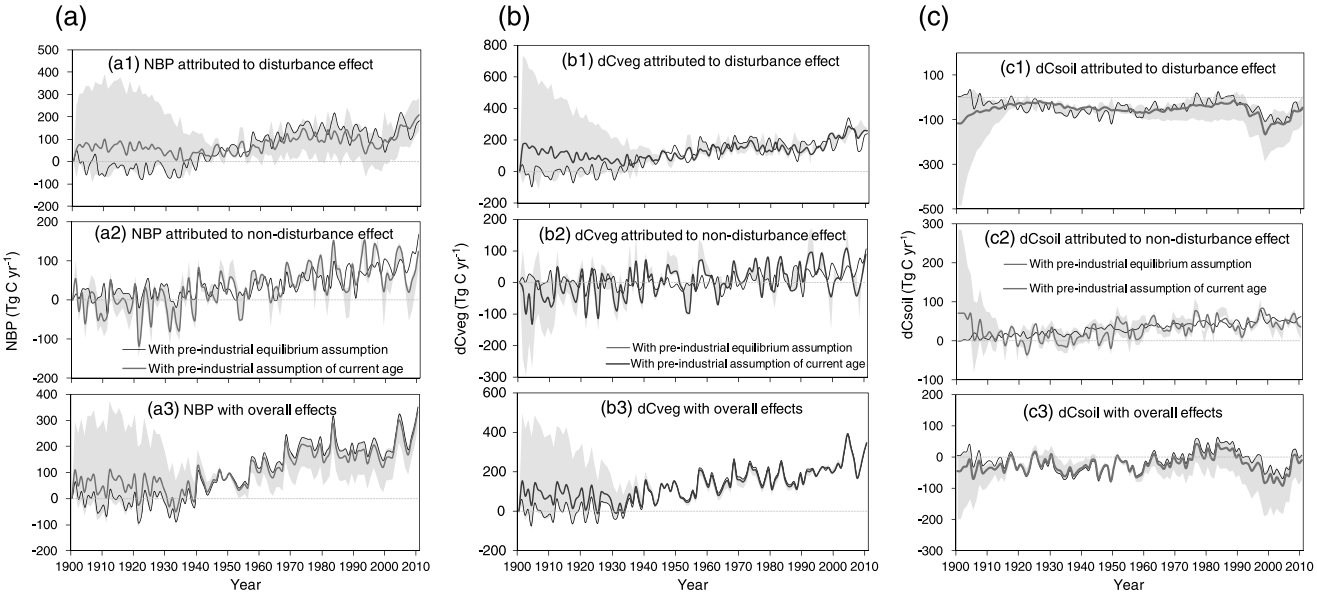

Figure 6. Modeled net biome productivity (NBP) and its living biomass (dCveg) and soil (dCsoil; nonliving biomass) components for conterminous U.S. forests in the period from 1901 to 2010. The shaded areas represent the uncertainty ranges from equilibrium assumptions. Positive values indicate C sinks, and negative values indicate C sources to the atmosphere.

Table 2. Absolute Errors (σ, Tg C yr^{-1}) and Relative Errors (e, %) of the 1951–2010 NBP and Its Living Biomass (dCveg) and Soil (dCsoil; Nonliving Biomass) Due To Equilibrium Assumptions for Forests With Unknown Stand Ages

	dCveg	dCsoil	NBP
Nondisturbance effect	3(12%)	3(8%)	3(4%)
Disturbance effect	6(4%)	21(−56%)[a]	27(21%)
Overall effect	6(3%)	18(613%)[a]	25(13%)

[a]Due to small value of dCsoil in Table 1, it seems that e was superlarge. Due to interaction of disturbance and nondisturbance effects on C changes, the overall uncertainty is not equal to the summation of uncertainties from each variable.

age became zero and stands started to regrow in the following year after disturbance until they were disturbed again by the most recent disturbances. If forests were not disturbed, they aged until they were disturbed again by the most recent disturbances.

The standard deviation of stand age ranged from 10 years in the eastern U.S. to 50 years in the western U.S. [*Pan et al*., 2011b]. To assess such effects, we adjusted the stand ages by ±5 years on average to each cell grid for the conterminous U.S. and studied their effects on the regional and continental NBP.

We also included the relative uncertainties in the reference NPP from the BEPS model [*Zhang et al*., 2012b] and the 18 NPP-age curves that were obtained from the FIA data [*He et al*., 2012].

Uncertainties from climate inputs and N deposition were evaluated by the method of *Williams et al*. [2012]:

$$S = \frac{\Delta C}{C}\frac{P}{\Delta P}, \tag{15}$$

where S is called the response coefficient and defined as the relative change in dependent variable caused by a relative change in a parameter (P). The negative (or positive) S means that the amplitude of NBP is dampened (or amplified). $|S| < 0.2$ represents no significance. For sensitivity analyses, we exercised NBP responses to a ±1% change of climates and N deposition.

Each of the sensitivity experiments was performed on the conterminous U.S. forests from 1901 to 2010, while our presentation of results mainly focused on the period from 1951 to 2010.

3. Results and Discussions

3.1. National C Sink and Source Estimation

On average during the period of 1951–2010, the total NBP of forests in the conterminous U.S. was 188 ± 60 Tg C yr^{-1} with 185 ± 56 Tg C yr^{-1} in the forest living biomass component and 3 ± 23 Tg C yr^{-1} in the forest soil component (Table 1). In the year with disturbances, most of Cveg will be released to the atmosphere, and the soil C pool will be reduced, which will result in a negative dCsoil. The main C sinks were found in the North and Pacific Southwest regions (Figure 5a) (Forest regions, described below, were based on U.S. Resources Planning Act (RPA) forest regions, http://www.fs.fed.us/research/rpa/regions.php.). The contribution to the C sink in the north region was mostly from forest regrowth effects, while it was from both regrowth and nondisturbance effects in the Pacific Southwest regions (Figures 5b and 5c). The C release due to disturbance events in disturbance years was about 68 ± 55 Tg C yr^{-1} on average from 1951 to 2010, which was mainly from the south region (Figure 5d).

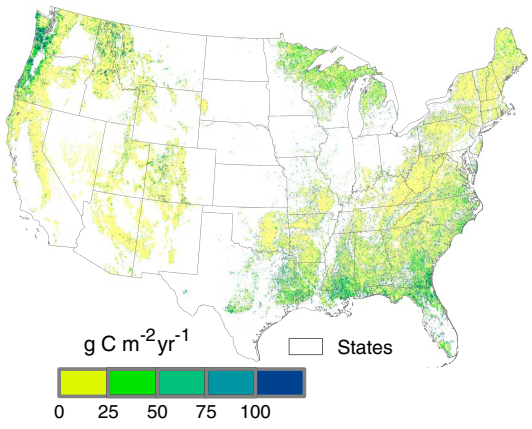

Figure 7. Spatial distributions of possible errors (standard deviation) in net biome productivity (NBP) in conterminous U.S. forests averaged from 1951 to 2010 due to equilibrium assumptions for forests with unknown stand ages.

3.1.1. Effects of Equilibrium Assumptions on NBP

The random assignments of age for forests with unknown stand age affected the simulations of subsequent NBP from 1901 to 2010, but the effects diminished after 1950 (our reporting period) because the fraction of forests with known stand age and

Table 3. Absolute Errors (σ, Tg C yr^{-1}) and Relative Errors (e, %) of the 1951–2010 NBP due to Uncertainties in Reference NPP, Stand Age, and NPP-Age Curves[a]

Uncertainty Sources	NBP Attributed to Nondisturbance Effects	NBP Attributed to Disturbance Effects	Overall NBP
Reference NPP	2(4%)	2(1%)	3(1%)
Stand age	12(21%)	32(26%)	53(28%)
NPP-age curves	3(5%)	18(14%)	15(8%)

[a]Due to interaction of disturbance and nondisturbance effects on C changes, the overall uncertainty is not equal to the summation of uncertainties from each variable.

disturbances histories increased with time (Figure 6 and Table 2). When all forests with unknown stand age were assigned an age of 20 years in the initial year (1900), the simulated NBP for conterminous U.S. forests was modified the most compared with using the equilibrium assumption or the other disequilibrium age assumptions. Since the assigned stand ages increased above 20 years, the influences of disequilibrium age assumptions on NBP decreased. If forests with unknown stand age were assumed to have the current stand ages (in 2006) in the initial year (1900), the averaged NBP for 1951–2010 was 12% lower than that under the equilibrium age assumptions, in which the NBP attributed to the disturbance effect was 20% lower. The influences of different disequilibrium assumptions in the model initial year were mainly embodied in the disturbance effect on NBP (Figure 6a). Analysis based on the spatial distribution of absolute error of NBP (Figure 7) showed that the uncertainties were the largest in the Southeast U.S. (including Georgia and Florida) and the Northwest U.S. (including Washington and Oregon) where most forests are young (<50 years) in 2010 and recently disturbed. In these areas, the historical disturbance and stand age information before 1950 was scarce.

The relative effect of the disequilibrium assumptions on the NBP component in living C biomass (dCveg) was smaller (<20%) than on the soil C component (dCsoil) from 1951 to 2010, especially after 1990 (within 10% differences compared to the equilibrium assumption) (Figure 6b). Conversely, the effect of disequilibrium assumptions on the overall dCsoil was much larger, as high as 200% different (Figure 6c), mainly resulting from the induced errors in simulating disturbance effects on dCsoil (Figure 6c). The disequilibrium assumptions, however, had small effects on the shares of dCveg and dCsoil that were related to nondisturbance factors from 1951 to 2010.

Results of the uncertainty analysis indicated that the overall uncertainty in the total NBP produced by the equilibrium assumption was within 13% for the 1951–2010 simulation, an acceptable uncertainty for a large-scale modeling exercise. However, the disequilibrium age assumptions generated significantly greater uncertainty in the simulated NBP prior to 1950 in those supposedly disturbed stands. Our uncertainty analyses highlight the importance of better historical stand age and disturbance data for improving historical C dynamics simulations, although the retention of the historical data in the early twentieth century may have less influence on the simulation of C dynamics in recent decades.

3.1.2. Effects on NBP From Uncertainties in NPP, Stand Age, and NPP-Age Curves

Among various sources of uncertainties including the reference NPP, stand age, and NPP-age curves, the uncertainty of the reference NPP did not change NBP greatly (<5%), while uncertainties in the stand age map and stand age curves resulted in relatively large differences in the simulated NBP from 1951 to 2010 (5%–28%) (Table 3). Specifically, the uncertainty in estimated stand age resulted in a difference of 53 Tg C yr^{-1} (28%) in the total NBP, composed of 32 Tg C yr^{-1} (26%) uncertainty from the disturbance effects on NBP. On the other hand, the uncertainty in NPP-age curves introduced differences of 14% and 5% in the disturbance and nondisturbance effects on the total NBP

Table 4. Absolute Errors (σ, Tg C yr^{-1}) and Relative Errors (e, %) of the 1951–2010 Carbon (C) Changes in Living Biomass (dCveg) due to Errors in Reference NPP, Stand Age, and NPP-Age Curves[a]

Uncertainty Sources	dCveg Attributed to Nondisturbance Effects	dCveg Attributed to Disturbance Effects	Overall dCveg
Reference NPP	2(11%)	1(1%)	3(1%)
Stand age	5(24%)	25(15%)	42(23%)
NPP-age curves	4(19%)	24(15%)	20(11%)

[a]Due to interaction of disturbance and nondisturbance effects on C changes, the overall uncertainty is not equal to the summation of uncertainties from each variable.

As for the living biomass component (dCveg), the uncertainty in reference NPP resulted in an 11% difference in dCveg attributed to the nondisturbance effect but the overall

Table 5. Absolute Errors (σ, Tg C yr^{-1}) and Relative Errors (e, %) of the 1951–2010 Carbon (C) Changes in Soil (dCsoil; Nonliving Biomass) due to Errors in Reference NPP, Stand Age, and NPP-Age Curves

Uncertainty Sources	dCsoil Attributed to Nondisturbance Effects	dCsoil Attributed to Disturbance Effects	Overall dCsoil
Reference NPP	0.1(0.3%)	0.1(0.3%)	0.1(5%)
Stand age	8(22%)	4(11%)	9(270%)[a]
NPP-age curves	1(3%)	10(27%)	10(333%)[a]

[a]Due to small value of dCsoil (3 ± 23 Tg C yr^{-1}) in Table 1, it seems that e was superlarge. Due to interaction of disturbance and nondisturbance effects on C changes, the overall uncertainty is not equal to the summation of uncertainties from each variable.

dCveg was only subject to a small difference (1%) (Table 4). The uncertainties in both stand age and NPP-age curves resulted in relatively large uncertainties (15%–24%) in dCveg components attributed to disturbance and nondisturbance effects, which further caused large uncertainties on the overall dCveg.

Since the soil component of NBP (dCsoil, 3 Tg C yr^{-1} on average) was extremely small compared to dCveg (185 Tg C yr^{-1} on average) during the period of 1951–2010, even small uncertainties in dCsoil could lead to higher relative changes in dCsoil, for instance, the uncertainties in stand age and NPP-age curves caused 270% and 333% of differences respectively in the dCsoil estimates although the absolute changes in dCsoil were small (9–10 Tg C yr^{-1}) (Table 5). The uncertainties in reference NPP had relatively small effects on dCsoil ($\leq$5%), while the uncertainties in stand age and NPP-age curves had relative large effects. Uncertainties in stand age changed dCsoil by 22% and 11%, respectively, relative to nondisturbance and disturbance effects, whereas the uncertainties in NPP-age curves had alternative impacts of 3% versus 27%.

In general, NBP simulations depend on the predisturbance C pools, and changes in soil C pools also have time lag effects. As a result, the changes in NPP, stand age, and NPP-age curves may produce asymmetric errors in biomass and soil components of NBP. The impact of stand age in this study was obviously greater than the impact of NPP-age curves on total NBP and dCveg, while the opposite effects of these two factors were bestowed to dCsoil. Because the forest stand age in the conterminous U.S. ranges broadly from ~10 to 900 years, the nonlinearity of NBP in response to stand age indicates that our estimates cannot be easily adjusted to correct the biases introduced by stand age and NPP-age curves.

3.1.3. Sensitivity of NBP to Climate and N Deposition

Results showed that the response coefficients of NBP variables to N changes were less than 0.2 (except for the dCsoil response to the decrease in N), suggesting that uncertainties in N deposition estimates do not propagate large biases in modeled NBP (Table 6). Changes in precipitation and temperature can influence the amplitude of NBP by changing NPP and R_h. Due to nonlinear functions of carbon uptake and release against temperature and water availability [*Canadell et al*., 2007; *Chmura et al*., 2011; *Reich et al*., 2014], response coefficients to precipitation and temperature varied differently by region. As for precipitation, the total dCveg showed a positive response coefficient while the total dCsoil showed a negative one for the conterminous U.S., resulting in a positive response of the total NBP. Conversely, the total dCveg showed a negative response while dCsoil showed a positive response, resulting in a partly negative response of the total NBP because climate warming induces a GPP increase that is less than the corresponding respiration increase (the magnitude of dCsoil is smaller). The analysis suggests that a 1% bias in climate variables will deliver ~0.53% to 1.53% biases in the amplitude of NBP of conterminous U.S. forests for the period of 1951–2010.

Table 6. Sensitivity Results of Net Biome Productivity (NBP) of Conterminous U.S. Forests to Climate Variables and N Deposition (N_{dep}) During the Period of 1951–2010[a]

Response Coefficients	dCveg	dCsoil	NBP
N_{dep}	0.01	0.27	0.05
Precipitation	1.37	−1.4	1.05
Temperature	−1.19	1.21	−0.89

[a]Results are expressed as the response coefficient (S) [*Williams et al*., 2012] and the equivalent change in NBP (Tg C yr^{-1}) caused by a 1% increase in the chosen parameter. The response coefficients are in percentage (%), and negative values indicate a response of NBP that depresses them toward zero. For example, "−0.05" represents a 0.05% decrease relative to the original results, due to a 1% change in parameters. NBP is equal to the sum of carbon (C) changes in living biomass (dCveg) and soil (dCsoil; nonliving biomass) components.

3.1.4. Propagated Uncertainties on Recent NBP

Comparing simulations with equilibrium assumptions in *Zhang et al*. [2012a] (Table 7), the equilibrium assumptions changed the stand age and disturbance distributions in forest areas lacking stand age and disturbance data. As a result, changes

Table 7. Effects of Disturbance and Nondisturbance Factors on Net Biome Productivity (NBP) (Tg C yr^{-1}) in Conterminous U.S. Forests During the Period of 1951–2010 With Total Absolute Errors due to Uncertainties of All Factors and the Absolute Errors due to the Equilibrium Assumptions[a]

	1991–2000	2001–2010	1991–2010	1951–2010
C release	−77 ± 65(7)	−66 ± 87(5)	−72 ± 58(6)	−68 ± 55(8)
Regrowth	208 ± 43(12)	227 ± 76(10)	217 ± 51(11)	194 ± 33(11)
Total disturbance effect	130 ± 95(33)	161 ± 83(30)	145 ± 87(31)	126 ± 60(27)
Total nondisturbance effect	85 ± 3(3)	70 ± 11(11)	78 ± 7(7)	58 ± 5(5)
NBP	215 ± 95(30)	231 ± 83(25)	223 ± 88(28)	188 ± 60(25)

[a]Numbers (Tg C yr^{-1}) in parentheses are propagated absolute errors (Tg C yr^{-1}) in NBP that resulted from equilibrium assumptions for forests with unknown stand ages. Disturbance effects are integrated effects of C release due to disturbance events and regrowth from stand age, while nondisturbance effects are integrated effects from climate, CO_2, and nitrogen deposition (N_{dep}). Due to interaction of disturbance and nondisturbance effects on C changes, the overall uncertainty is not equal to the summation of uncertainties from each variable.

in stand age distribution directly affected forest regrowth patterns, while changes in disturbance patterns influenced the regrowth patterns after disturbance events and C release to the atmosphere. Results showed that the equilibrium assumptions propagated 25 Tg C yr^{-1} to the total uncertainties (60 Tg C yr^{-1}) in simulating the pre-1950 NBP. The propagated uncertainties in NBP were mainly embodied in the disturbance effects on NBP. Conversely, these assumptions did not affect post-1950 C release greatly, where uncertainties were mostly attributed to the accuracy of input data after 1950. However, these assumptions resulted in 20% difference in the post-1950 regrowth contributions to NBP, which would be attributed to the large forest areas with unknown stand age prior to 1950. For nondisturbance effects on NBP, these equilibrium assumptions had a smaller impact.

3.1.5. Recent National C Sink and Source Estimation

In the 1990s, C sinks were mostly found in the Mid-Atlantic and Lake States while C sources occurred in the northern West Coast, Rocky Mountain, and south regions (Figure 8a). In the 2000s, C sink areas expanded to the south region (especially coastal areas) where it became the largest C sink. Conversely, some sinks in the Rocky Mountain regions shifted to small C sources (Figure 8b). On average from 1991 to 2010, C sinks were found in the eastern U.S. and southern West Coast regions (Figure 9a), and the increase of C sinks was primarily from forest regrowth effects (Figure 9b). Although the enhancement effects from nondisturbance factors increased forest C sequestered across the U.S. forests (Figure 9c), it was overwhelmed by the negative regrowth effect in the early recovery stage and C release due to disturbance factors in the northern West Coast and Rocky Mountain regions, resulting in C sources in these areas. In contrast, the south region was becoming a large C sink in 2000s that was attributed to the strong regrowth effects when forests got into more productive ages (Figure 9b), although C release from disturbance events was the largest among the regions (Figure 9d).

Overall, comparing the individual factors contributing to the average NBP (Table 7), the regrowth effect on NBP was more important than other effects. The largest contribution of regrowth to NBP was situated in the north region during the period of 1951–2010, while a strong regrowth effect also occurred in both the north and south regions during the period of 1991–2010. Both CO_2 and N deposition exerted positive effects on NBP,

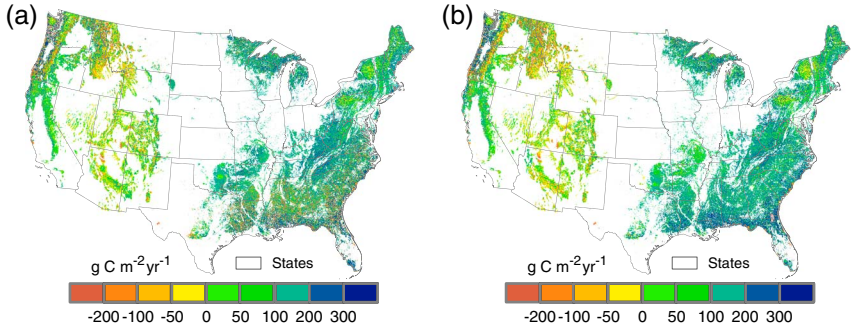

Figure 8. Spatial distribution of net biome productivity (NBP) in conterminous U.S. forests in the 1990s and 2000s (Positive values indicate sinks of C, and negative values indicate sources of C to the atmosphere.).

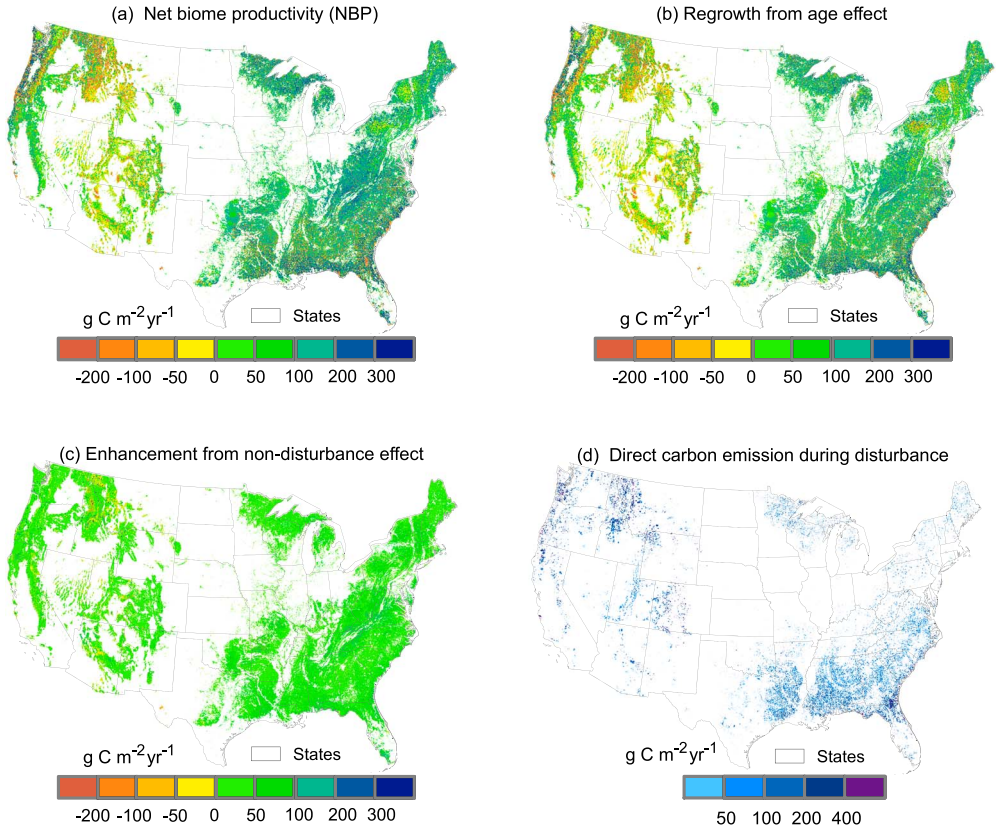

Figure 9. Same as Figure 5 but for the period from 1991 to 2010.

whereas the effect of CO_2 increased productivity more than that of N deposition [*Zhang et al.*, 2012a]. Changes in climate increased the average NBP from 1951 to 2010 but produced a negative effect from 1991 to 2010.

3.2. Limitations

Our current C estimates did not account for C fluxes in forestland converted to nonforestland. Such areas account for ~0.3% yr^{-1} since 1951 based on the FIA data [*Birdsey and Lewis*, 2002]. Although we did not account for land use change in this study, the net effects of deforestation and afforestation over the last 50 years have been about neutral since the total area of forests in the U.S. has not changed significantly. There is little difference in NEP between these two classes, and they are small relative to C changes in biomass [*Smith et al.*, 2006]. The overall accuracy for classification of conterminous U.S. for forest-type groups is 69% although the map was based on the explicit FIA data [*Ruefenacht et al.*, 2008]. It is difficult to accurately identify the differences in C estimates due to misclassified forest types for the conterminous U.S., and this deserves further exploration in the future. The model excludes C fluxes of understory vegetation (e.g., grass and short shrub), which may play a role to compensate the C loss in the early stage of forest regrowth and further result in underestimation of C accumulation. It is also important to account for the negative impacts of tropospheric ozone on forest productivity [*Pan et al.*, 2009], but this effect is not yet included in our model.

4. Conclusion

This analysis examines uncertainties caused by equilibrium age assumptions in initializing models, and uncertainties of other input variables, expanding our previous study on C changes and C attributions of disturbance and nondisturbance factors in U.S. forests for 1901–2010 [*Zhang et al.*, 2012a]. Using disequilibrium assumptions for forests with unknown stand age and disturbance information, we further investigated whether the equilibrium assumptions for these forests in years of the early twentieth century (1901–1950) could affect the estimation of C changes in conterminous U.S. forests from 1951 to 2010. The results indicated that the largest uncertainties in estimated NBP were from inadequate information about stand ages in some forests

prior to 1950. Uncertainties in nondisturbance factors had relatively small influences on the total NBP with differences within 10%. On the other hand, uncertainties in disturbance-related factors resulted in 4%–28% differences in the total NBP. Since the disturbance information and stand age were less known prior to 1950, the equilibrium assumptions of forest stand age affected greatly the simulated results on C sinks or sources in the pre-1950 period but much less in the post-1950 results. We therefore conclude that even though the forest disturbance data are lacking before 1950, the forest C dynamics in the recent decades (1951–2010) can be simulated within 13% with the pre-1950 disturbance effects based on a dynamic equilibrium assumption for forest stands with unknown age.

Our analysis also reveals that regrowth effects contributed more to C sinks in the northeastern U.S. after 1950 than before 1950. On average from 1951 to 2010, C release due to disturbances was the largest in the southeastern U. S., but this region became the largest C sink due to the contribution of regrowth after 2000. In contrast, some significant parts of the west became C sources after 2000 due to increasing disturbance and climate effects.

Appendix A

Supplementary data associated with this article can be found in the supporting information.

A1. Equations for Calculating ΔC_x

The equations used to describe C changes in disturbed and nondisturbed years are updated from *Chen et al*. [2000, 2000a, 2000b], *Ju et al*. [2007], and *Govind et al*. [2011].

$$\Delta C_l(i) = \left\{f_l \mathrm{NPP}(i) - k_{l,\mathrm{smd}} C_l(i-1) - k_{l,\mathrm{ssd}} C_l(i-1) - \xi_l C_l(i-1)\right\} / \left[1 + k_{l,\mathrm{smd}} + k_{l,\mathrm{ssd}} + \xi_l\right] \quad \text{(A1)}$$

$$\Delta C_w(i) = \left\{f_w \mathrm{NPP}(i) - k_{w,\mathrm{cd}} C_w(i-1) - \xi_w C_w(i-1)\right\} / \left[1 + k_{w,\mathrm{cd}} + \xi_w\right] \quad \text{(A2)}$$

$$\Delta C_{\mathrm{cr}}(i) = \left\{f_{\mathrm{cr}} \mathrm{NPP}(i) - k_{\mathrm{cr,cd}} C_{\mathrm{cr}}(i-1) - \xi_{\mathrm{cr}} C_{\mathrm{cr}}(i-1)\right\} / \left[1 + k_{\mathrm{cr,cd}} + \xi_{\mathrm{cr}}\right] \quad \text{(A3)}$$

$$\Delta C_{\mathrm{fr}}(i) = \left\{f_{\mathrm{fr}} \mathrm{NPP}(i) - k_{\mathrm{fr,fmd}} C_{\mathrm{fr}}(i-1) - k_{\mathrm{fr,fsd}} C_{\mathrm{fr}}(i-1) - \xi_{\mathrm{fr}} C_{\mathrm{fr}}(i-1)\right\} / \left[1 + k_{\mathrm{fr,fmd}} + k_{fr,\mathrm{fsd}} + \xi_{\mathrm{fr}}\right] \quad \text{(A4)}$$

$$\begin{aligned}\Delta C_{\mathrm{cd}}(i) = \big\{&(1-\xi_w) k_{w,\mathrm{cd}} C_w(i) + (1-\xi_{\mathrm{cr}}) k_{\mathrm{cr,cd}} C_{\mathrm{cr}}(i) - \xi_{\mathrm{cd}} C_{\mathrm{cd}}(i-1) \\ &- \Lambda(i)(1-\xi_{\mathrm{cd}})\left(k_{\mathrm{cd},a} + k_{\mathrm{cd},m} + k_{\mathrm{cd},s}\right) C_{\mathrm{cd}}(i-1)\big\} / \left[1 + \Lambda(i)\left(k_{\mathrm{cd},a} + k_{\mathrm{cd},m} + k_{\mathrm{cd},s}\right)\right]\end{aligned} \quad \text{(A5)}$$

$$\begin{aligned}\Delta C_{\mathrm{fsd}}(i) = \big\{&(1-F_m(i))(1-\xi_{\mathrm{fr}}) k_{\mathrm{fr,fsd}} C_{\mathrm{fr}}(i) \\ &- \Lambda(i)\left(k_{\mathrm{fsd},a} + k_{\mathrm{fsd},m} + k_{\mathrm{fsd},s}\right) C_{\mathrm{fsd}}(i-1)\big\} / \left[1 + \Lambda(i)\left(k_{\mathrm{fsd},a} + k_{\mathrm{fsd},m} + k_{\mathrm{fsd},s}\right)\right]\end{aligned} \quad \text{(A6)}$$

$$\begin{aligned}\Delta C_{\mathrm{ssd}}(i) = \big\{&(1-F_m(i))(1-\xi_l) k_{l,\mathrm{ssd}} C_l(i) - \xi_{\mathrm{ssd}} C_{\mathrm{ssd}}(i-1) \\ &- \Lambda(i)(1-\xi_{\mathrm{ssd}})\left(k_{\mathrm{ssd},a} + k_{\mathrm{ssd,sm}} + k_{\mathrm{ssd},s}\right) C_{\mathrm{ssd}}(i-1)\big\} / \left[1 + \Lambda(i)\left(k_{\mathrm{ssd},a} + k_{\mathrm{ssd,sm}} + k_{\mathrm{ssd},s}\right)\right]\end{aligned} \quad \text{(A7)}$$

$$\begin{aligned}\Delta C_{\mathrm{fmd}}(i) = \big\{&F_m(i)(1-\xi_{\mathrm{fr}}) k_{\mathrm{fr,fmd}} C_{\mathrm{fr}}(i) - \xi_{\mathrm{fmd}} C_{\mathrm{fmd}}(i-1) \\ &- \Lambda(i)\left(k_{\mathrm{fmd},a} + k_{\mathrm{fmd},m}\right) C_{\mathrm{fmd}}(i-1)\big\} / \left[1 + \Lambda(i)\left(k_{\mathrm{fmd},a} + k_{\mathrm{fmd},m}\right)\right]\end{aligned} \quad \text{(A8)}$$

$$\begin{aligned}\Delta C_{\mathrm{smd}}(i) = \big\{&F_m(i)(1-\xi_l) k_{l,\mathrm{md}} C_l(i) - \xi_{\mathrm{smd}} C_{\mathrm{smd}}(i-1) \\ &- \Lambda(i)(1-\xi_{\mathrm{smd}})\left(k_{\mathrm{smd},a} + k_{\mathrm{smd,sm}}\right) C_{\mathrm{smd}}(i-1)\big\} / \left[1 + \Lambda(i)\left(k_{\mathrm{smd},a} + k_{\mathrm{smd,sm}}\right)\right]\end{aligned} \quad \text{(A9)}$$

$$\Delta C_{\mathrm{sm}}(i) = \left\{\Lambda(i)\left(k_{\mathrm{smd},m} C_{\mathrm{smd}}(i) + k_{\mathrm{ssd},m} C_{\mathrm{ssd}}(i)\right) - \Lambda(i) k_{m,s} C_{sm}(i-1)\right\} / \left[1 + \Lambda(i) k_{m,s}\right] \quad \text{(A10)}$$

$$\begin{aligned}\Delta C_m(i) = \big\{&\Lambda(i)\left(k_{\mathrm{cd},m} C_{\mathrm{cd}}(i) + k_{\mathrm{fsd},m} C_{\mathrm{fsd}}(i) + k_{\mathrm{fmd},m} C_{\mathrm{fmd}}(i) + k_{s,m} C_s(i) + k_{p,m} C_p(i-1)\right) \\ &- \left[\Lambda(i)\left(k_{m,a} + k_{m,s}\right) + k_{m,p}\right] C_m(i-1)\big\} / \left[1 + \Lambda(i)\left(k_{m,a} + k_{m,s}\right) + k_{m,p}\right]\end{aligned} \quad \text{(A11)}$$

$$\begin{aligned}\Delta C_s(i) = \big\{&\Lambda(i)\left(k_{\mathrm{cd},s} C_{\mathrm{cd}}(i) + k_{\mathrm{fsd},s} C_{\mathrm{fsd}}(i) + k_{m,s} C_m(i) + k_{\mathrm{sm},s} C_{\mathrm{sm}}(i) + k_{\mathrm{ssd},s} C_{\mathrm{ssd}}(i)\right) \\ &- \left[\Lambda(i)\left(k_{s,a} + k_{s,m}\right) + k_{s,p}\right] C_s(i-1)\big\} / \left[1 + \Lambda(i)\left(k_{s,a} + k_{s,p} + k_{s,m}\right)\right]\end{aligned} \quad \text{(A12)}$$

$$\Delta C_p(i) = \left\{k_{s,p} C_s(i) + k_{m,p} C_m(i) - \Lambda(i)\left[k_{p,a} + k_{p,m}\right] C_p(i-1)\right\} / \left[1 + \Lambda(i)\left(k_{p,a} + k_{p,m}\right)\right] \quad \text{(A13)}$$

Table A1. Carbon (C) Allocation Coefficients of Net Primary Productivity (NPP) to Biomass C Pools Used in the InTEC Model[a]

No.	NPP Allocation	Fate	Allocation Rate		
			Coniferous	Deciduous	Mixed
	f_l		0.2129	0.2326	0.2077
	f_w		0.3010	0.4024	0.3317
	f_{fr}		0.3479	0.2160	0.2770
	f_{cr}		0.1482	0.1590	0.1836

[a] f_l, f_w, f_{fr}, and f_{cr} represent NPP allocation rates to foliage, wood, fine root, and coarse root, respectively.

Notation

Symbol	Definition
f_x	NPP allocation coefficient to pool x;
ξ_x	C loss from C pool x due to disturbance events;
$k_{x,y}$	C transfer rate from C pool x to C pool y;
C_x	C content in C pool x;
F_m	partitioning fraction of leaf and fine root litters to metabolic detritus C pool;
Λ	abiotic decomposition factor.

Subscript Notation

l, w, cr, fr	foliage, wood, coarse root, fine root;
cd, fsd, fmd,	woody litter, soil structural detritus, soil metabolic detritus;
m, s, sm, ssd	soil microbe, slow, surface microbe, surface structural detritus;
smd, p, a	surface metabolic detritus, passive, atmosphere.

A2. Parameters for InTEC

The parameters used to describe C allocation, turnover rates, decomposition rates, and loss rate in the InTEC model are listed in Tables A1, A2, A3. These rates were based on empirical data and plant functional types, derived from literature.

A3. AmeriFlux Eddy Covariance Data Used

The AmeriFlux network provides invaluable eddy covariance (EC) data (http://ameriflux.ornl.gov). In its Level 4 product, a number of continuous records of half-hourly net ecosystem exchange (NEE) were gap filled using the marginal distribution sampling method [*Reichstein et al.*, 2005] or the artificial neural network method [*Papale and Valentini*, 2003]. NEE estimates were aggregated from half-hourly data to monthly and yearly values. In this study, the 147 site-year NEEs at 35 AmeriFlux sites across U.S. (Figure A1 and Table A4) representing a diversity of forest ecosystems and climate types were used for validating NEP estimates. Stand age shown here was the actual age in 2006.

Table A2. Turnover Rates and Carbon (C) Loss Rates in Fire From Biomass C Pools Defined in the InTEC Model[a]

No.	Biomass C Pools	Fate	Turnover Rates			Loss Rate in Fire ξ_{fx}
			Coniferous	Deciduous	Mixed	
1	C_l	C_{ssd}, C_{smd}	0.1925	1.0000	0.3945	1
2	C_w	C_{cd}	0.0249	0.0288	0.0279	0.25
3	C_{fr}	C_{fsd}, C_{fmd}	0.5948	0.5948	0.5948	0
4	C_{cr}	C_{cd}	0.0229	0.0448	0.0268	0

[a] C_l, C_w, C_{fr}, C_{cr}, C_{ssd}, C_{smd}, C_{cd}, C_{fsd}, and C_{fmd} represent the C pool of foliage, wood, fine root, coarse root, surface structural detritus, surface metabolic detritus, woody litter, soil structural detritus, and soil metabolic detritus, respectively.

Table A3. Decomposition Rates of Soil Carbon (C) Pools and C Loss Rate in Fire Defined in the InTEC Model[a]

No.	Soil C Pools	Fate	Decomposition Rate	Loss rate in fire ξ_{fx}
1	C_{smd}	C_{sm}, C_a	$k_{smd,sm} = 0.4KN_{ssd}(i)A(i)$ $k_{smd,a} = 0.6KN_{ssd}(i)A(i)$	1
2	C_{ssd}	C_s, C_{sm}, C_a	$k_{ssd,sm} = 0.4KN_{ssd}(i)f_{ssd,sm}(LC_l)$ $k_{ssd,s} = 0.7KN_{ssd}(i)f_{ssd,s}(LC_l)$ $k_{ssd,a} = 0.6KN_{ssd}(i)f_{ssd,sm}(LC_l) + 0.3KN_{ssd}(i)f_{ssd,s}(LC_l)$	1
3	C_{sm}	C_s, C_a	$k_{sm,s} = 0.4A(i)$ $k_{sm,a} = 0.6A(i)$	
4	C_{cd}	C_m, C_s, C_a	$k_{cd,m} = 0.45KN_{cd}(i)f_{cd,m}(LC_w, , LC_{cr})A(i)$ $k_{cd,s} = 0.7KN_{cd}(i)f_{cd,s}(LC_w, , LC_{cr})A(i)$ $k_{cd,a} = 0.55KN_{cd}(i)f_{cd,m}(LC_w, , LC_{cr})A(i) + 0.3KN_{cd}(i)f_{cd,s}(LC_w, , LC_{cr})A(i)$	1
5	C_{fmd}	C_m, C_a	$k_{fmd,m} = 0.45KN_{fmd}(i)A(i)$ $k_{fmd,a} = 0.55KN_{fmd}(i)A(i)$	
6	C_{fsd}	C_s, C_m, C_a	$k_{fsd,m} = 0.45KN_{fsd}(i)f_{fsd,m}(LC_{fr})$ $k_{fsd,s} = 0.7KN_{fsd}(i)f_{fsd,s}(LC_{fr})$ $k_{fsd,a} = 0.55KN_{fsd}(i)f_{fsd,m}(LC_{fr}) + 0.3f_{fsd,s}(LC_{fr})$	
7	C_m	C_p, C_s, C_a	$k_{m,s} = 7.3f_{m,s}(T_m)A(i)$ $k_{m,p} = 7.3f_{m,p}(T_m)A(i)$ $k_{m,a} = 7.3f_{m,a}(T_m)A(i)$	
8	C_s	C_m, C_p, C_a	$k_{s,m} = 0.25f_{s,m}(T_m)A(i)$ $k_{s,p} = 0.25f_{s,p}(T_m)A(i)$ $k_{s,a} = 0.19A(i)$	
9	C_p	C_m, C_a	$k_{p,m} = 0.003A(i)$ $k_{p,a} = 0.003A(i)$	

[a] $A(i)$ is the integrated annual abiotic effects of soil temperature and moisture in year i; $f_{x,y}(T_m)$ is a scalar for the effect of soil texture (T_m); $KN_x(i)$ is a scalar for the effect of N availability; $f_{x,y}(LC_z)$ is the impact of lignin content (LC). C_{cd}, C_{fsd}, C_{fmd}, C_m, C_s, C_{sm}, C_{ssd}, C_{smd}, C_p, and C_a represents C pool of woody litter, soil structural detritus, soil metabolic detritus, soil microbe, slow, surface microbe, surface structural detritus, surface metabolic detritus, passive, and the atmosphere, respectively.

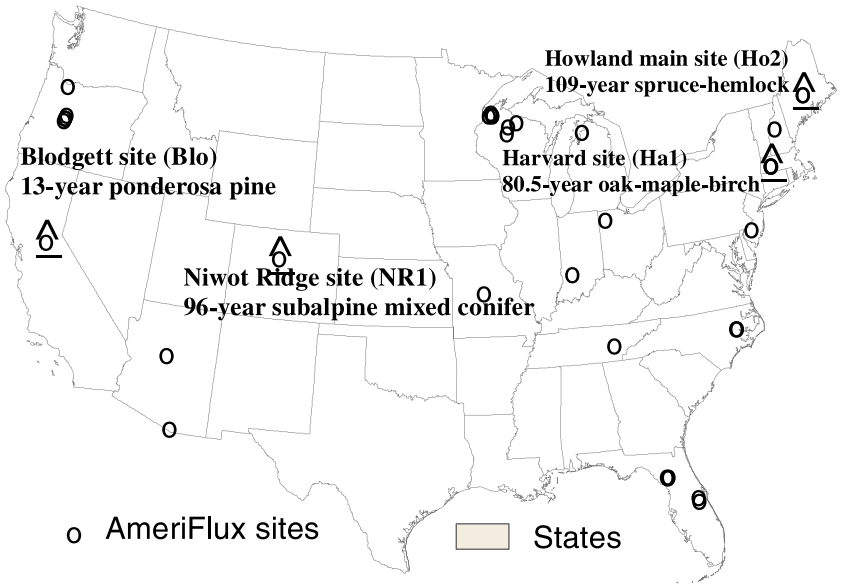

Figure A1. Spatial distribution of the 35 AmeriFlux forest sites used in this study.

Table A4. Summary of the Actual Attributes of 35 AmeriFlux Tower Used in This Study[a]

CEIP-ID	Latitude (Deg)	Longitude (Deg)	Actual Age (Years)	Actual Land Cover	Actual Forest Type	Forest Age Map (Years)
Wi4	46.7393	91.1663	70 in 2009	ENF	1	51/18
Wi7	46.6491	91.0693	>5 in 2009	shrub	1	3
Wi6	46.6249	91.2982	9 in 2009	shrub	11	40
Wi0	46.6188	91.0814	15 in 2009	ENF	4	16/60
Syv	46.242	89.3476	350 in max	MF	8	58
Los	46.0827	89.9792	>45	shrub	17	46/59
Wrc	45.8205	121.9519	450–500	ENF	5	50/71
WCr	45.8059	90.0799	55–90	DBF	15	31/52
UMB	45.5598	84.7138	79 (mean	DBF	16	78/48
Ho2	45.2091	68.747	109	ENF	7	91
Ho1	45.2041	68.7402	109	ENF	7	91
Me1	44.5794	121.5	59 (mean)/110 (max) in 2003	ENF	6	59
Me2	44.4523	121.5574	56 (mean)/89 (max) in 2004	ENF	6	50
Me5	44.4372	121.5668	22 (mean)/30 (max) in 2008	ENF	19	50
Me3	44.3154	121.6078	18 (max) in 2004	ENF	6	88
Bar	44.0646	71.2881	99	DBF	15	102
LPH	42.5419	72.185	47 in 2005	DBF	11	43/83
Ha2	42.5393	72.1779	100–230	ENF	9	43/83
Ha1	42.5378	72.1715	80.5	DBF	15	43/83
Oho	41.5545	83.8438	45 (mean)	DBF	12	50
NR1	40.0329	105.5464	98 (2008)	ENF	1	98/167
Dix	39.9712	74.4345	73 in 2005	MF	11	61
MMS	39.3232	86.4131	70 (mean)	DBF	16	65/83
Blo	38.8952	120.6328	6–7 in 2000	ENF	6	4/9
MOz	38.7441	92.2	77 (mean)	DBF	12	45
WBW	35.9588	84.2874	50–120	DBF	12	61/100
NC1	35.8115	76.7115	5	ENF	4	22
NC2	35.8031	76.6679	18	ENF	4	22
Fuf	35.089	111.762	~100	ENF	6	61
SRM	31.8214	110.8661	60	Savanna	19	0
SP2	29.7648	82.2448	10 in 2009	ENF	3	3
SP3	29.7548	82.1633	18 in 2008	ENF	3	9
SP1	29.7381	82.2188	80 (mean)	ENF	3	46
KS2	28.6086	80.6715	14 in 2010	shrub	11	18/29
KS1	28.4583	80.6709	15 in 2010	ENF	3	30/36

[a]1: White/Red/Jack Pine; 2: Spruce; 3: Longleaf/Slash Pine; 4: Loblolly/Shortleaf Pine; 5: Douglas-fir; 6: Ponderosa; 7: Fir/Spruce/Mountain Hemlock; 8: Lodgepole Pine; 9: Hemlock/Sitka Spruce; 10: California Mixed Conifer; 11: Oak/Pine; 12: Oak/Hickory; 13: Oak/Gum/Cypress; 14: Elm/Ash/Cottonwood; 15: Maple/Beech/Birch; 16: Aspen/Birch; 17: Alder/Maple; and 18: Western Oak. DBF: deciduous boardleaf forest; ENF: evergreen coniferous forest; and MF: mixed forest.

Acknowledgments

We greatly appreciate the availability of the annual tower flux data from the AmeriFlux network sites. We are greatly indebted to the principle investigators of AmeriFlux and their research teams operating the 35 forest sites selected for our model validation. Thanks are also extended to Eric Sundquist and two anonymous reviewers for providing constructive comments during the review process. The research is supported by a research grant from National and Jiangsu Natural Science Funds for Young Scholar (31300420, 41105078, and BK20130987) and USDA Forest Service Research grant (07-JV-11242300-114). Data and models to support this article are from the research collaboration of Jingming Chen at University of Toronto with the U.S. Forest Service. Please contact fmin.zhang@utoronto.ca for additional information about this study.

References

Adams, D. M., R. W. Haynes, and A. J. Daigneault (2006), Estimated timber harvest by U.S. region and ownership, 1950–2002, General Technical Report PNW-GTR-659, Pacific Northwest Research Station, U.S. Department of Agriculture, Forest Service, Portland, Oreg.

Birdsey, R. A., and L. S. Heath (1995), Carbon changes in U.S. forests, in *Productivity of America's Forests and Climate Change*, General Technical Report RM-GTR-271, U.S. Department of Agriculture, Forest Service, Fort Collins, Colo.

Birdsey, R. A., and G. M. Lewis (2002), Current and historical trends in use, management and disturbance of United States forest lands, in *The Potential of U.S. Forest Soils to Sequester Carbon and Mitigate the Greenhouse Effect*, edited by J. Kimble et al., CRC Press, Boca Raton, Fla.

Birdsey, R. A., and G. M. Lewis (2003), Carbon in U.S. forests and wood products, 1987–1997: State-by-state estimates, General Technical Report NE-310, U.S. Department of Agriculture, Forest Service, Newtown Square, Pennsylvania.

Boerner, R. E. J., J. Huang, and S. C. Hart (2008), Fire, thinning, and the carbon economy: Effects of fire and fire surrogate treatments on estimated carbon storage and sequestration rate, *For. Ecol. Manage.*, doi:10.1016/j.foreco.2007.11.021.

Bradford, J. B., and D. N. Kastendick (2010), Age-related patterns of forest complexity and carbon storage in pine and aspen-birch ecosystems of northern Minnesota, USA, *Can. J. For. Res.*, *40*, 401–409.

Canadell, J. G., C. Le Quéré, M. R. Raupach, B. F. Christopher, E. T. Buitenhuis, P. Ciais, T. J. Conway, N. P. Gillett, R. A. Houghton, and G. Marland (2007), Contributions to accelerating atmospheric CO_2 growth from economic activity, carbon intensity, and efficiency of natural sinks, *Proc. Natl. Acad. Sci. U.S.A.*, *104*, 18,866–18,870.

Carvalhais, N., M. Reichstein, G. J. Collatz, M. D. Mahecha, M. Migliavacca, C. S. R. Neigh, E. Tomelleri, A. A. Benali, D. Papale, and J. Seixas (2010), Identification of vegetation and soil carbon pools out of equilibrium in a process model via eddy covariance and biometric constraints, *Global Change Biol.*, *16*, 2813–2829, doi:10.1111/j.1365-2486.2010.02173.x.

Chen, J. M., J. Liu, J. Cihlar, and M. L. Goulden (1999), Daily canopy photosynthesis model through temporal and spatial scaling for remote sensing applications, *Ecol. Modell.*, *124*, 99–119.

Chen, J. M., W. Chen, J. Liu, and J. Cihlar (2000), Annual carbon balance of Canada's forests during 1895–1996, *Global Biogeochem. Cycles*, *14*(3), 839–850, doi:10.1029/1999GB001207.
Chen, W., J. M. Chen, and J. Cihlar (2000a), Integrated terrestrial ecosystem carbon-budget model based on changes in disturbance, climate, and atmospheric chemistry, *Ecol. Modell.*, *135*, 55–79.
Chen, W., J. M. Chen, J. Liu, and J. Cihlar (2000b), Approaches for reducing uncertainties in regional forest carbon balance, *Global Biogeochem. Cycles*, *14*(3), 827–838, doi:10.1029/1999GB001206.
Chen, J. M., W. Ju, J. Cihlar, D. Price, J. Liu, W. Chen, J. Pan, A. Black, and A. Barr (2003), Spatial distribution of carbon sources and sinks in Canada's forests, *Tellus*, *55B*, 622–641.
Chmura, D. J., P. D. Anderson, G. T. Howe, C. A. Harrington, J. E. Halofsky, D. L. Peterson, D. C. Shaw, and J. B. S. Clair (2011), Forest responses to climate change in the northwestern United States: Ecophysiological foundations for adaptive management, *For. Ecol. Manage.*, *261*, 1121–1142.
Environmental Protection Agency (EPA) (2009), Inventory of U.S. greenhouse gas emissions and sinks: 1990–2007, EPA 430-R-09–004.
Farquhar, G. D., S. von Caemmerer, and J. A. Berry (1980), A biochemical model of photosynthetic CO_2 assimilation in leaves of C_3 species, *Planta*, *149*, 78–90.
Flato, G. M., and G. J. Boer (2001), Warming asymmetry in climate change simulations, *Geophys. Res. Lett.*, *28*, 195–198, doi:10.1029/2000GL012121.
Govind, A., J. M. Chen, P. Bernier, H. Margolis, L. Guindon, and A. Beaudoin (2011), Spatially distributed modeling of the long-term carbon balance of a boreal landscape, *Ecol. Model.*, doi:10.1016/j.ecolmodel.2011.04.007.
Harris, I., P. D. Jones, T. J. Osborn, and D. H. Lister (2014), Updated high-resolution grids of monthly climatic observations—The CRU TS3.10 dataset, *Int. J. Climatol.*, *34*, 623–642.
He, L., J. M. Chen, S. Zhang, G. Gomez, Y. Pan, K. McCullough, R. A. Birdsey, and J. G. Masek (2011), Normalized algorithm for mapping and dating forest disturbances and regrowth for the United States, International, *J. Appl. Earth Obs. Geoinf.*, *13*(2), 236–245.
He, L., J. M. Chen, Y. Pan, and R. A. Birdsey (2012), Relationships between net primary productivity and forest stand age derived from Forest Inventory and Analysis data and remote sensing imagery, *Global Biogeochem. Cycles*, *26*, GB3009, doi:10.1029/2010GB003942.
Hurtt, G. C., S. W. Pacala, P. R. Moorcroft, J. Caspersen, E. Shevliakova, R. A. Houghton, and B. Moore III (2002), Projecting the future of the U.S. carbon sink, *Proc. Natl. Acad. Sci. U.S.A.*, *99*(3), 1389–1394, doi:10.1073/pnas.012249999.
Ince, P. J. (2000), Industrial wood productivity in the United States, 1900–1998. Research Note FPL-RN-0272, Madison, WI: Forest Service, United States Department of Agriculture, Forest Products Laboratory.
Ju, W., and J. M. Chen (2005), Distribution of soil carbon stocks in Canada's forests and wetland simulated based on drainage class, topography and remote sensing, *Hydrol. Processes*, *19*, 77–94.
Ju, W. M., J. M. Chen, D. Harvey, and S. Wang (2007), Future carbon balance of China's forests under climate change and increasing CO_2, *J. Environ. Manage.*, *85*, 538–562, doi:10.1016/j.jenvman.2006.04.028.
Kasischke, E. S., K. P. O'Neill, N. H. F. French, and L. L. Bourgeau-Chavez (2000), Controls on patterns of biomass burning in Alaska boreal forests, in *Fire, Climate Change and Carbon Cycling in the Boreal Forest*, edited by E. S. Kasischke and B. J. Stocks, pp. 173–196, Springer, New York.
Keeling, R. F., S. C. Piper, A. F. Bollenbacher, and S. J. Walker (2009), Atmospheric CO_2 records from sites in the SIO air sampling network, in *Trends: A Compendium of Data on Global Change*, Carbon Dioxide Inf. Anal. Cent., Oak Ridge Natl. Lab., U.S. Dep. of Energy, Oak Ridge, Tenn., doi:10.3334/CDIAC/atg.035.
Kurz, W. A., C. C. Dymond, G. Stinson, G. J. Rampley, E. T. Neilson, A. L. Carroll, T. Ebata, and L. Safranyik (2008), Mountain pine beetle and forest carbon feedback to climate change, *Nature*, *452*, 987–990.
Masek, J. G., and G. J. Collatz (2006), Estimating forest carbon fluxes in a disturbed southeastern landscape: Integration of remote sensing, forest inventory, and biogeochemical modeling, *J. Geophys. Res.*, *111*, G01006, doi:10.1029/2005JG000062.
Masek, J. G., C. Huang, R. Wolfe, W. Cohen, F. Hall, J. Kutler, and P. Nelson (2008), North American forest disturbance mapped from a decadal Landsat record, *Remote Sens. Environ.*, *112*, 2914–2926, doi:10.1016/j.rse.2008.02.010.
Morales-Nin, B., S. C. Swan, J. D. M. Gordon, M. Palmer, A. J. Geffen, T. Shimmield, and T. Sawyer (2005), Age-related trends in otolith chemistry of Merluccius merluccius from the north-eastern Atlantic Ocean and the western Mediterranean Sea, *Mar. Freshwater Res.*, *56*, 1–9.
Pan, Y., B. Richard, J. Hom, and K. McCullough (2009), Separating effects of changes in atmospheric composition, climate and land-use on carbon sequestration of U.S, *For. Ecol. Manage.*, *259*, 151–164.
Pan, Y., et al. (2011a), A large and persistent carbon sink in the world's forests, *Science*, *333*, 988–993.
Pan, Y., J. M. Chen, R. A. Birdsey, K. McCullough, L. He, and F. Deng (2011b), Age structure and disturbance legacy of North American forests, *Biogeosciences*, *8*, 715–732.
Papale, D., and R. Valentini (2003), A new assessment of European forests carbon exchanges by eddy fluxes and artificial neural network spatialization, *Global Change Biol.*, *9*, 525–535.
Parton, W. J., D. S. Schimel, C. V. Cole, and D. S. Ojima (1987), Analysis of factors controlling soil organic matter levels in Great Plains grasslands, *Soil Sci. Soc. Am. J.*, *51*, 1173–1179.
Pietsch, S. A., and H. Hasenauer (2006), Evaluating the self-initialization procedure for large-scale ecosystem models, *Global Change Biol.*, *12*, 1658–1669.
Reich, P. B., S. E. Hobbie, and T. D. Lee (2014), Plant growth enhancement by elevated CO_2 eliminated by joint water and nitrogen limitation, *Nature Geosci.*, doi:10.1038/NGEO2284.
Reichstein, M., J. A. Subke, A. C. Angeli, and J. D. Tenhunen (2005), Does the temperature sensitivity of decomposition of soil organic matter depend upon water content, soil horizon, or incubation time?, *Global Change Biol.*, *11*, 1754–1767.
Ruefenacht, B., et al. (2008), Conterminous U.S. and Alaska forest type mapping using forest inventory and analysis data, *Photogramm. Eng. Remote Sens.*, *74*(11), 1379–1388.
Running, S. W. (2008), Ecosystem disturbance, carbon, and climate, *Science*, *321*, 652–653.
Schimel, D., et al. (2000), Contribution of increasing CO_2 and climate to carbon storage by ecosystems in the United States, *Science*, *287*, doi:10.1126/science.287.5460.2004.
Smith, J. E., L. S. Heath, K. E. Skog, and R. A. Birdsey (2006), Methods for calculating forest ecosystem and harvested carbon with standard estimated for forest types of the united States, General Technical Report NE-343, Washington, DC: United States Department of Agriculture, Forest Service, Northeastern Research Station.
Smith, W. B., P. D. Miles, C. H. Perry, and S. A. Pugh (2009), Forest resources of the United States, 2007: A technical document supporting the Forest Service 2010 RPA assessment, General Technical Report WO-78, Washington, DC: United States Department of Agriculture, Forest Service, Washington Office.
Taylor, J. R. (1997), *An Introduction to Error Analysis: The Study of Uncertainties in Physical Measurements*, 2nd ed., Univ. Sci. Books, Sausilito, Calif.

Thornton, P. E., and S. W. Running (1999), An improved algorithm for estimating incident daily solar radiation from measurements of temperature, humidity, and precipitation, *Agric. Forest Meteorol.*, *93*, 211–228.

Townsend, A. R., B. H. Braswell, E. A. Holland, and J. E. Penner (1996), Spatial and temporal patterns in potential terrestrial carbon storage resulting from deposition of fossil fuel derived nitrogen, *Ecol. Appl.*, *6*, 806–814.

Turner, D. P., G. J. Koerper, M. E. Harmon, and J. J. Lee (1995), A carbon budget for forests of the conterminous United States, *Ecol. Appl.*, *5*(2), 421–436, doi:10.2307/1942033.

Weng, E. S., and Y. Q. Luo (2011), Relative information contributions of model vs. data to short- and long-term forecasts of forest carbon dynamics, *Ecol. Appl.*, *21*(5), 1490–1505.

Wiedinmyer, C., and J. C. Neff (2007), Estimates of CO_2 from fires in the United States: Implications for carbon management, *Carbon Balance Manage.*, *2*, 10, doi:10.1186/1750-0680-2-10.

Williams, C. A., G. J. Collatz, J. Masek, and S. N. Goward (2012), Carbon consequences of forest disturbance and recovery across the conterminous United States, *Global Biogeochem. Cycles*, *26*, GB1005, doi:10.1029/2010GB003947.

Wutzler, T., and M. Reichstein (2007), Soils apart from equilibrium—Consequences for soil carbon balance modelling, *Biogeosciences*, *4*, 125–136.

Zeng, H., J. Q. Chambers, R. I. Negrn-Juarez, G. C. Hurtt, and D. B. Baker (2009), Impacts of tropical cyclones on U.S. forest tree mortality and carbon flux from 1851–2000, *Proc. Natl. Acad. Sci. U.S.A.*, *106*(19), 7888–7892.

Zhang, F. M., J. M. Chen, Y. Pan, R. A. Birdsey, S. H. Shen, W. Ju, and L. He (2012a), Attributing carbon sinks in conterminous U.S. forests to disturbance and non-disturbance factors from 1901 to 2010, *J. Geophys. Res.*, *117*, G02021, doi:10.1029/2011JG001930.

Zhang, F. M., J. M. Chen, J. Q. Chen, C. M. Goughd, T. A. Martine, and D. Dragonif (2012b), Evaluating spatial and temporal patterns of MODIS GPP over conterminous U.S. against flux measurements and a process model, *Remote Sens. Environ.*, *124*, 717–729, doi:10.1016/j.rse.2012.06.023.

Zscheischler, J., et al. (2014), Impact of large-scale climate extremes on biospheric carbon fluxes: An intercomparison based on MsTMIP data, *Global Biogeochem. Cycles*, *28*, 585–600, doi:10.1002/2014GB004826.